Received: 7 January 2022 | Revised: 21 May 2022 | Accepted: 29 June 2022

IET Generation, Transmission & Distribution

DOI: 10.1049/gtd2.12575

The Institution of Engineering and Technology WILEY

ORIGINAL RESEARCH

A nonlinear adaptive excitation controller design for two-axis models of synchronous generators in multimachine power systems to augment the transient stability during severe faults

Tushar Kanti Roy[1] | **Md Apel Mahmud**[2]

[1]Department of Electronics & Telecommunication Engineering, Rajshahi University of Engineering & Technology, Rajshahi, Bangladesh

[2]Faculty of Engineering & Environment, Northumbria University Newcastle, Newcastle Upon Tyne, UK

Correspondence
Tushar Kanti Roy, Department of Electronics, and Telecommunication Engineering, Rajshahi University of Engineering & Technology, Rajshahi 6204, Bangladesh.
Email: tkroy@ete.ruet.ac.bd

Abstract

This paper presents an excitation controller design process for multimachine power systems with synchronous generators using an adaptive backstepping approach to ensure robust performance against parametric uncertainties as well as to improve the transient stability during large disturbances. In this work, electrical dynamics of synchronous generators are described using two-axis models while excitations systems are represented as the IEEE Type II exciter which mainly captures electrical dynamics while swing equations are used to capture mechanical dynamics. The proposed adaptive backstepping control approach is then employed to derive the excitation control law. The proposed adaptive backstepping scheme uses all nonlinearities, which are mainly due to the interconnections and rotations of rotors in synchronous generators, within the dynamical models to improve the transient stability during severe disturbances. Furthermore, this excitation control scheme uses estimated values of parameters appearing in the dynamical models of power system which are estimated using adaptation laws based on real-time measurements and hence, it provides robustness against parametric uncertainties. The theoretical stability of the proposed scheme is assessed using the Lyapunov stability theory, that is, by checking the negative definiteness or semi-definiteness of the derivative of control Lyapunov functions (CLFs). Rigorous simulations are conducted on an IEEE 39-bus 10-machine test power system for evaluating the performance of the proposed scheme under different operating conditions. Simulation results clearly demonstrate the superiority of the adaptive backstepping excitation controller over existing nonlinear controllers including an existing adaptive backstepping excitation controller that is designed using the classical model of synchronous generators.

1 | INTRODUCTION

Excitation controllers paly a key role for augmenting the overall transient stability of power grids when these grids experience severe disturbances. Excitation controllers are mainly designed to deliver the desired damping toque into power systems during transient conditions. Since power systems exhibit continuously changing behaviors, excitation controllers must be capable to ensure the stability with changes in operating conditions and this needs to be considered while designing excitation controllers. Furthermore, the damping capability of excitation controllers directly depends on the parameters of synchronous generators and excitation systems along with the dynamical models as these parameters appear in the control signal [1]. Hence, the effects of such parameter variations and model accuracies also need to be considered while designing an excitation controller.

Power system stabilizers (PSSs) are traditional excitation controllers for synchronous generators in power systems which are utilized for enhancing transient stability under small disturbances [2, 3]. However, linearized models of transient level synchronous generators are used to design PSSs which do not

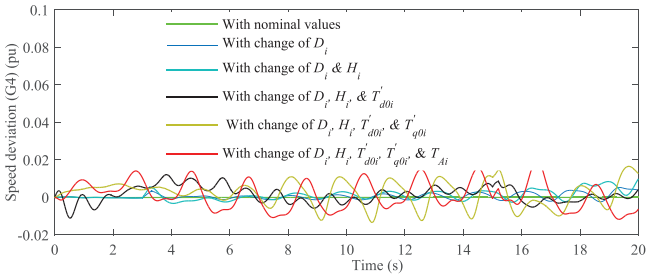

FIGURE 1 Speed deviation of G4 with variations in different parameters

have the ability to cope with large perturbations due to large disturbances within the network. Some advanced excitation linear control schemes are designed for synchronous generators with the assumption that there are only small variations in operating points. The examples of such linear excitation control schemes include the H_∞ scheme based on solving linear matrix inequalities (LMIs) and the linear quadratic regulator (LQR)-based approach that are designed using the solution of Riccati equations as discussed in [4, 5]. However, these linear excitation controller are still not capable to ensure the stable operation during the major grid events (e.g. sudden loss of generations due to short-circuit faults at their output terminal, sudden tripping of transmission lines etc.) despite their effectiveness under known upper and lower bounds of steady-state operating conditions. Moreover, the assumption for slight variations in operating point is valid when synchronous generators are used to supply base loads without any external faults which is not the general case as continuous changes in loads or faults are very obvious in modern power grids. Therefore, excitation controllers should be capable to manage the large disturbances under any operating conditions.

Nonlinear excitation controllers can be designed using nonlinear models of synchronous generators for ensuring the stable operation without relying on a fixed set of operating conditions. Different nonlinear controller design techniques such as the feedback linearization [6–8], adaptive backstepping [9, 10], and sliding mode [11, 12] approaches are generally used to determine excitation control inputs in conjunctions with different linear control techniques.

Three different feedback linearization techniques, for example, direct, exact, and partial feedback approaches are reported in the existing literature to design and implement excitation controllers in power networks [7, 13–15]. Direct and exact feedback linearization techniques use state and nonlinear coordinate transformation techniques, respectively, in order to linearize the nonlinear power system. With both of these approaches, the orders of the original nonlinear systems and transformed linear systems remain the same. As a result, the rotor angle (which is not available from the direct measurement) of synchronous generators needs to use as the feedback to implement the excitation control law obtained from direct and exact feedback linearization schemes. Therefore, additional observers are required for implementing these excitation controllers and such observers are not considered as cost-effective solutions [16]. The measurements of rotor angle associated with the implementation of the excitation controllers using direct and exact feedback linearization scheme can be overcome using partial feedback linearizing excitation controllers [15]. Moreover, the application of the partial feedback linearization technique simplifies the original power system model into a reduced-order one using nonlinear coordinate transformations which in turn makes the controller design process simple. However, the main problem associated with all these feedback linearizing excitation controllers is that these are designed using the transient level (i.e. one-axis) models of synchronous generators. Though a more realistic higher-order (two-axis) model is used in [17] to determine the excitation control input for synchronous generators using the obtain partial feedback linearization scheme, the performance of all these controllers are drastically affected if parameters appearing in the control law are slightly perturbed. Furthermore, the feedback linearization techniques cancel some useful nonlinearities of power systems.

Nonlinear excitation controllers using the sliding mode control technique ensure robustness against perturbed parameters including transient condition due to severe external disturbances [11, 12, 18]. These sliding mode excitation controllers are designed based on time-varying sliding surfaces whose selection process is complicated for synchronous generators represented by higher-order models. As a result, existing excitation controllers using the sliding mode control scheme are mostly designed using one-axis models of synchronous generators. However, the unmodeled dynamics of synchronous generators excite the responses during the transient events whose severity is more for large disturbances. Though an advanced synchronous generator model having a higher-order configuration is used in [19] to avoid the excitements arising from unmodeled dynamics, the responses exhibit huge chattering effects even with the cost of huge complexities during the implementation.

The adaptive backstepping control scheme can be considered as another straightforward and effective way to obtain the excitation control law which utilizes all nonlinearities in the system model and assists to avoid parameter sensitivity problems as well as steady-state chattering effects [20, 21]. Excitation controllers based on the adaptive backstepping approach guarantee the desired tracking of all states appearing in the dynamical model and dynamically adapt all parameters in the model as this approach has parameter adaptation features [22]. A neural network (NN)-based adaptive excitation control scheme is presented in [23] in which dynamic characteristics are estimated using a two-layer NN. However, the approach in [23] still uses the typical third-order dynamical model as the reference model. Similar models are used in [24–27] to design excitation controllers using an adaptive approach where the parameter adaptation includes only the estimation of the damping coefficient rather than all parameters appearing in the model. Since the damping coefficient is not only the parameter that affects the stable operation of power systems, these controllers are not capable to ensure the overall stability with perturbations in other parameters including the parameters of the excitation system

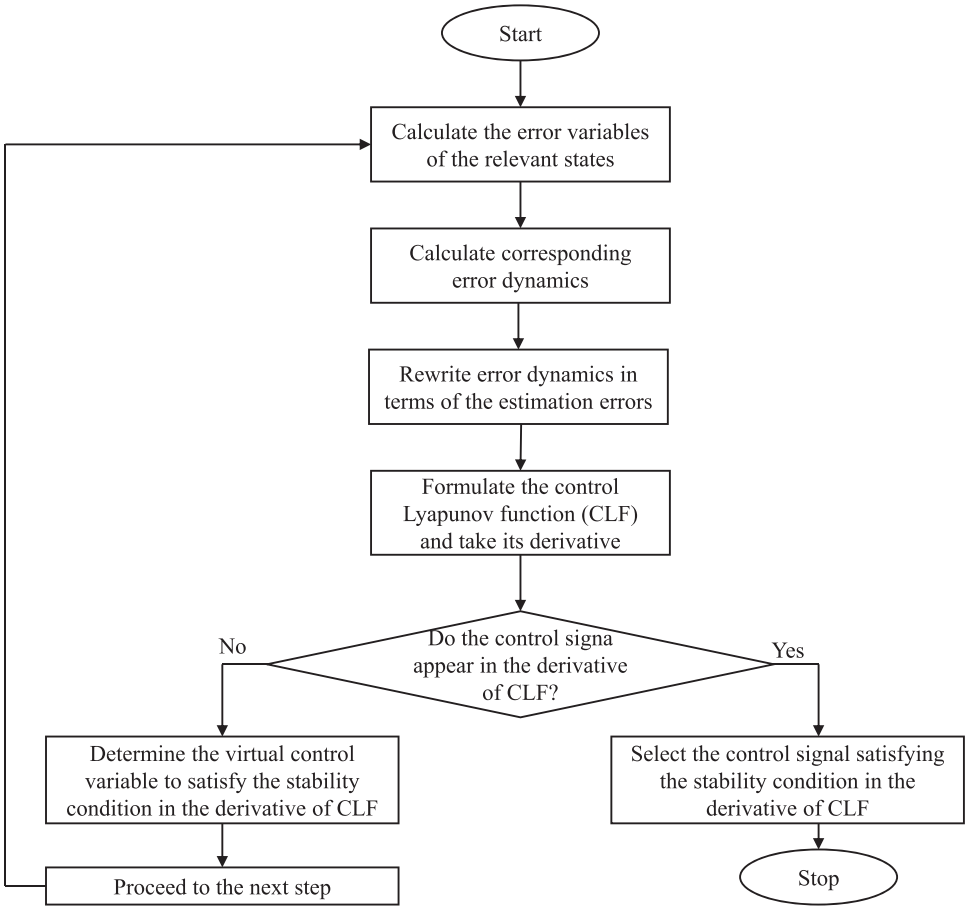

FIGURE 2 The overall flowchart of the proposed ABEC

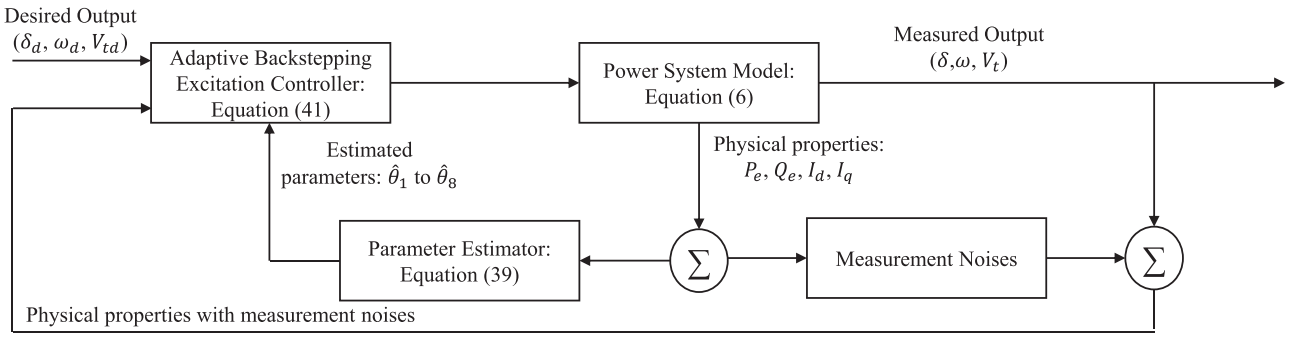

FIGURE 3 The implementation block diagram of the proposed control scheme

that are not considered in most of the existing literature so far presented here.

The adaptive excitation controller as presented in [28] estimates all parameters appearing within the dynamical model capturing dynamics of power systems where the synchronous generator is modeled as the classical third-order one with a first-order model of an IEEE Type II exciter. This model cannot accurately capture some useful dynamic characteristics of synchronous generators, for example, the terminal voltage of synchronous generators relies on the voltages of both direct- and quadrature-axis and the third-model only considers the dynamic of the quadrature-axis voltage. Hence, the excitation controller designed from such models (i.e. without having some important dynamics) will not be capable to enhance the stability [29]. This issue is resolved in [30] through a robust adaptive approach by incorporating the dynamic of direct-axis transient voltage in addition to the existing model used in [29]. The robust excitation controller in [30] estimates all parameters while modeling external disturbances in terms of measurement noises. The main problem of this robust excitation controller

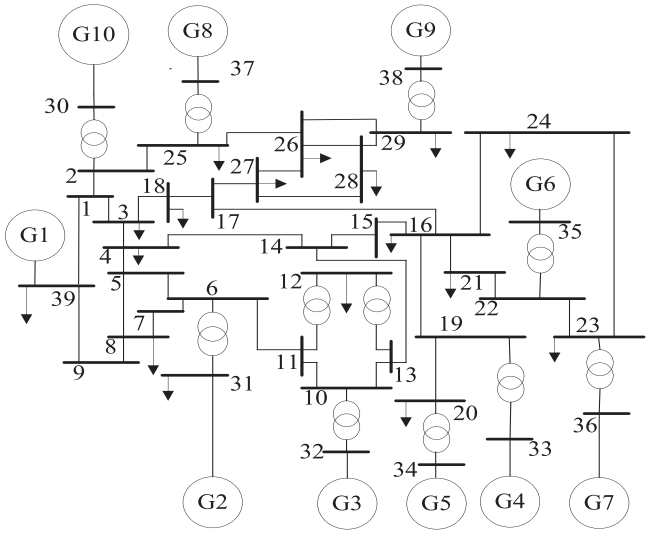

FIGURE 4 IEEE Test system (39-bus 10-machine) for assessing the performance of the ABEC

in [30] is that some known bound need to be imposed on external disturbances which in turn restrict the stability of power systems. The condition for bounding uncertainties can easily be avoided by inherent including the effects of external disturbances within the model. By considering this fact, an adaptive excitation controller is designed in [31] for the synchronous generator connected to an infinite bus where the generator is represented by the two-axis model. The controller in [31] also uses estimated values of key parameters in the model. However, synchronous generators exhibits different characteristics in real power systems which comprise more than a single generator. Moreover, the damping coefficients and inertia constants of synchronous generators are still considered as known in [30, 31] though these significantly disturb the stable operation of power systems. For this reason, it is essential to design an adaptive backstepping excitation controllers (ABEC) that will be capable to estimate all parameters for multiple synchronous generators in a power system and ensure the stability during severe transients.

The previous works based on the third-order model of synchronous generators a multimachine power system using a similar nonlinear adaptive backstepping approach mostly neglect the effects of the automatic voltage regulator though it plays a significant role in the voltage control. Hence, the existing works mostly ensure the angle stability by maintaining the synchronous speed and do not play any roles for the voltage control. The unique feature of the proposed scheme is the consideration of the dynamic of the automatic voltage regulator during the controller design process and the relevant parameter (e.g. time constant) as unknown. This is extremely important as the automatic voltage regulator continuously adjusts the terminal voltage which causes the variation in the time constant. The variation of this parame-

FIGURE 5 Terminal voltages with a symmetrical 3LG fault at the terminal of G4

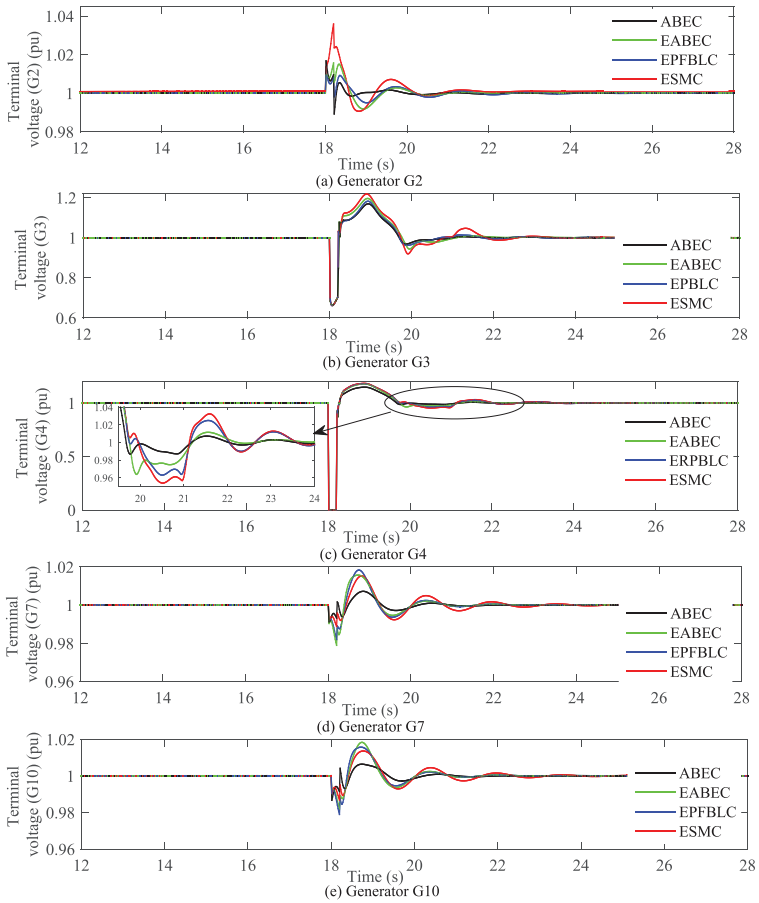

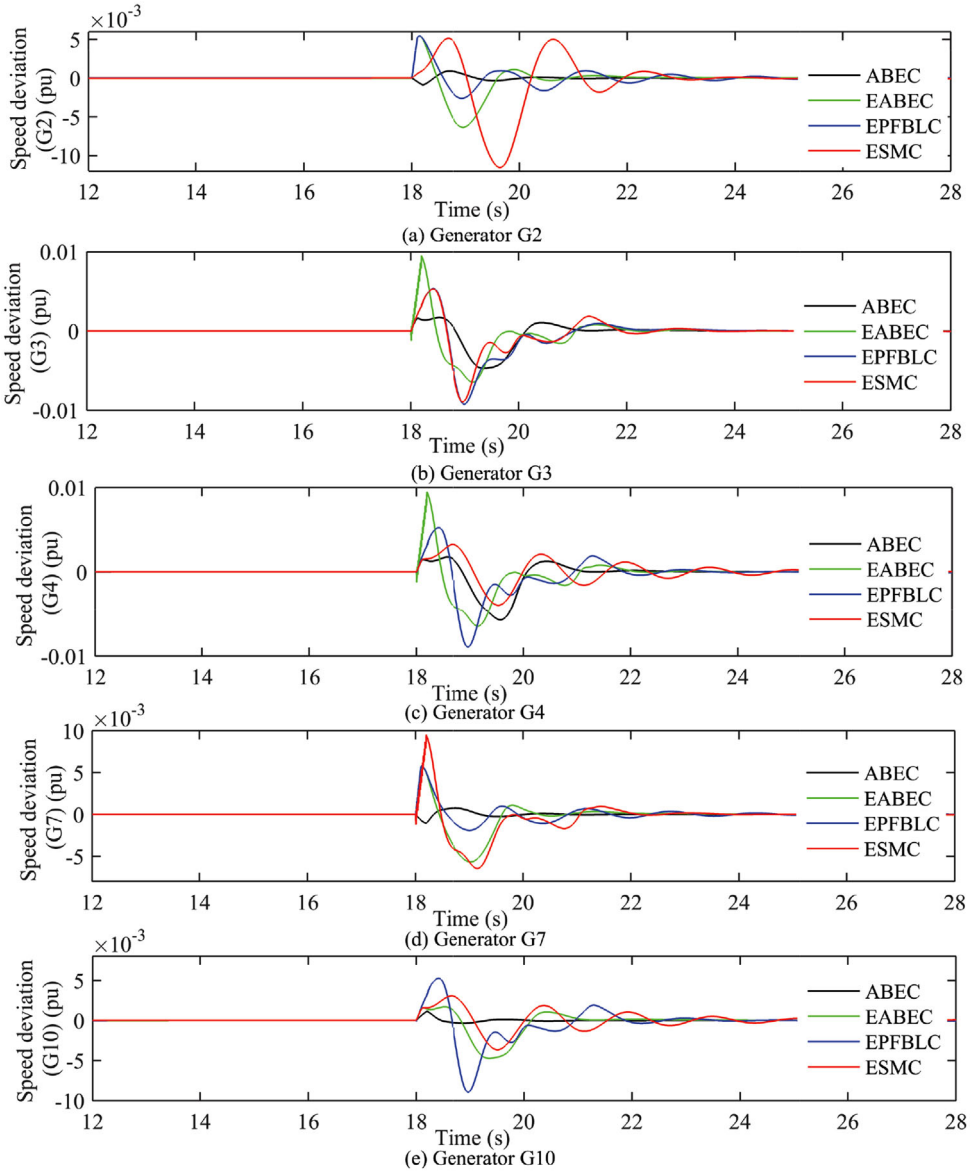

FIGURE 6 Speed deviations with a symmetrical 3LG fault at the terminal of G4

ter significantly affect the stability margin of power systems. Furthermore, this work considers a fast excitation system with the reduced-order fast dynamic model which are not considered in the existing backstepping controllers that use the third-order model of the synchronous generator. In this work, the ABEC in [31] is extended for multimachine power systems where the nonlinear dynamical models include the mechanical dynamics, electrical dynamics (for both direct- and quadrature-axis), and dynamics of excitation systems. The main novelty of the proposed scheme as compared to the approaches as presented in [9, 20–22, 27, 28, 30] are summarized in the following:

- The use of two-axis model for capturing electrical dynamics and guaranteeing the convergence of all states in the dynamical model to their desired values. The proposed adaptive backstepping control approach can handle both steady-state and transient stability effectively. It is well-known that the variations of stability sensitive parameters are very common in power systems and these parameters in real power system depend on the transient behaviors. Therefore, it is beneficial to consider parametric uncertainties in the synchronous generator and incorporate these during the controller design process. Thus, in such cases, an excitation controller needs to be designed in such a way that it not only stabilizes the nominal system at a desired equilibrium point but also guarantees robustness with respect to unknown parameter variations. In such cases, the adaptive controller can handle these parameter variations and quickly stabilize the transient behaviors.
- The adaptation of all parameters in the dynamical model without imposing any bounds. It is worth to note that all

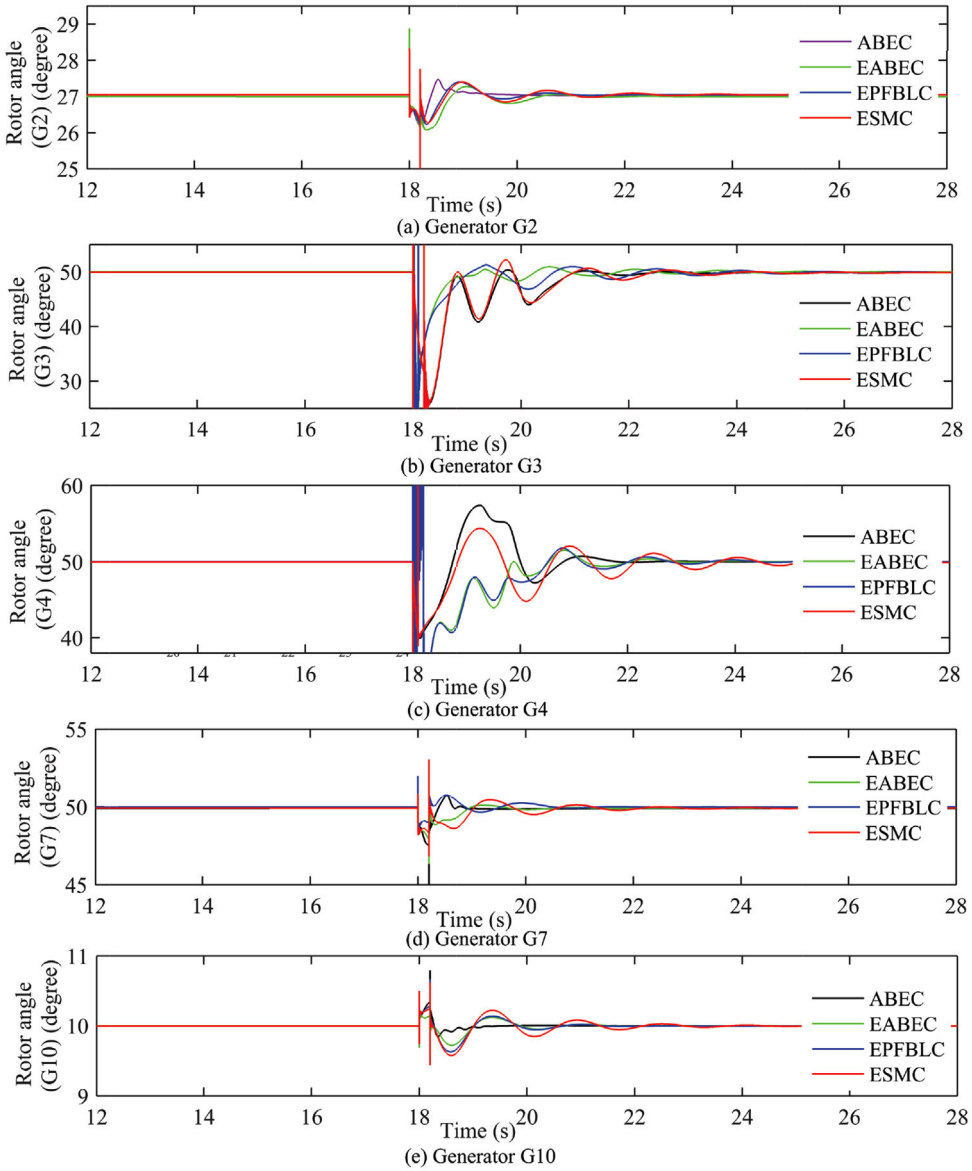

FIGURE 7 Rotor angles with a symmetrical 3LG fault at the terminal of G4

parameters have their own bounds for a real physical system and though the controller is designed for unbounded parameters, the simulations are carried out for around 10% variation in all parameters from their nominal values. Please note that the estimation of all parameters will not increase the overall complexity of the control law rather it will increase the number of the adaptation laws.

In the proposed scheme, adaptation laws are derived to estimate all parameters in the dynamical model of each synchronous generator and the newly proposed excitation control scheme uses these estimated values to guarantee the convergence of all states which in turn ensure the overall stability during major disturbances on power systems. The proposed ABEC does not neglect any nonlinearities within the power system model like other existing methods, for example, the feedback linearization scheme. This enables the controller to provide sufficient damping and the relevant control Lyapunov functions (CLFs) are formulated during each step of the controller design process for analyzing the theoretical stability. An IEEE test system having 39-bus and 10 synchronous generators, which is often known an New England power system, is used for validating the effectiveness of the proposed ABEC under different operating scenarios while applying large disturbances. The comparative results are also presented where these comparisons are made with an existing ABEC (EABEC), partial feedback linearizing, and sliding mode controllers.

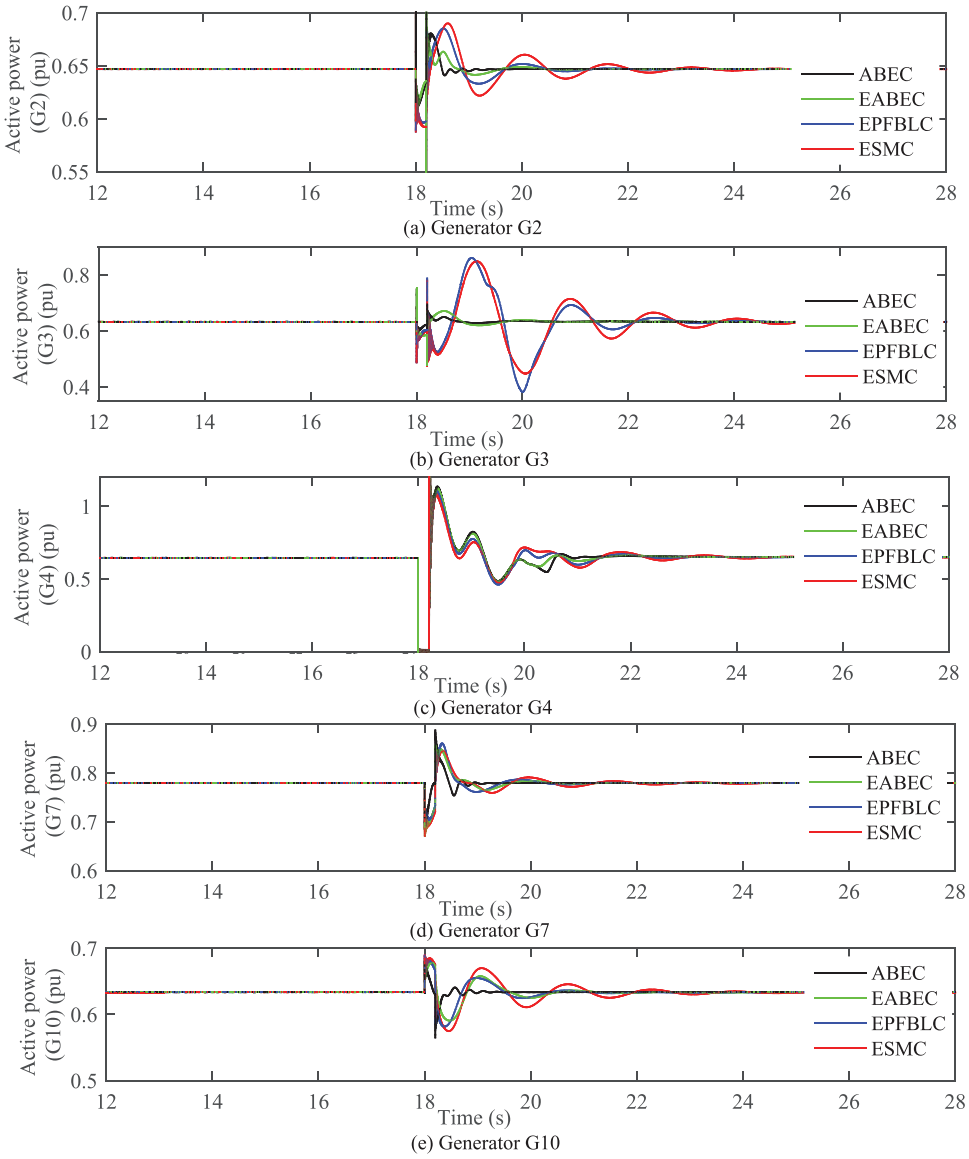

FIGURE 8 Output active power responses with a symmetrical 3LG fault at the terminal of G4

2 | DYNAMICAL MODEL OF SYNCHRONOUS GENERATORS IN POWER SYSTEMS

The dynamical model of multimachine power systems needs to be developed for deriving the excitation control signal. This section presents mechanical dynamics, electrical dynamics considering two-axis, and fast dynamic of the excitation system. The dynamics of synchronous generators dominate the operation of traditional power networks [2]. Since synchronous generators convert the mechanical power into electrical power, it is essential to consider both mechanical and electrical dynamics. The dynamical models are considered in a generalized way by considering N interconnected synchronous generators through transmission lines and transformers. In such a system, all synchronous generators exhibit similar dynamic behaviors where the effects of interconnections are captured through the power and current flowing through different parts of the system. Swing equations represent the mechanical dynamics which can be expressed through following two equations [17, 32]:

$$\begin{aligned}\dot{\delta}_i &= \omega_i - \omega_{0i} \\ \dot{\omega}_i &= -\frac{D_i}{2H_i}(\omega_i - \omega_{0i}) + \frac{\omega_{0i}}{2H_i}(P_{mi} - P_{ei})\end{aligned}. \tag{1}$$

The symbols in Equation (1) are defined in a similar way as presented in [17, 32]. For two-axis models of synchronous generators, the electrical dynamics of i^{th} synchronous generator can

be expressed as:

$$\begin{aligned}\dot{E}'_{qi} &= -\frac{1}{T'_{doi}}E'_{qi} - \frac{(x_{di}-x'_{di})}{T'_{doi}}I_{di} + \frac{1}{T'_{doi}}E_{fdi}\\ \dot{E}'_{di} &= -\frac{1}{T'_{qoi}}E'_{di} + \frac{(x_{qi}-x'_{qi})}{T'_{qoi}}I_{qi}\end{aligned}, \quad (2)$$

where symbols in Equation (2) can be defined in a way as discussed in [17, 32]. This work considers a fast excitation system and the reduced-order fast dynamic of such an exciter can be represented as [17, 32]:

$$\dot{E}_{fdi} = -\frac{E_{fdi}}{T_{Ai}} + \frac{K_{Ai}}{T_{Ai}}(\Delta V_i + V_{ci}), \quad (3)$$

where $\Delta V_i = V_{refi} - V_{ti}$ and symbols in Equation (3) can be defined in a similar manner as presented in [17, 32]. The relevant algebraic equations demonstrating the voltage-current relationship, that is, the effects of interconnections can be represented as [17, 32]:

$$\begin{aligned}&V_{di} = E'_{di} - R_{si}I_{di} + x'_{qi}I_{qi},\ V_{qi} = E'_{qi} - R_{si}I_{qi} + x'_{di}I_{di}\\ &V_{ti} = \sqrt{V_{di}^2 + V_{qi}^2}\\ &I_{di} = \sum_{j=1}^{n} Y_{ij}[E'_{di}\cos(\delta_{ij}+\theta_{ij}) - E'_{qi}\sin(\delta_{ij}+\theta_{ij})]\\ &I_{qi} = \sum_{j=1}^{n} Y_{ij}[E'_{qi}\cos(\delta_{ij}+\theta_{ij}) + E'_{di}\sin(\delta_{ij}+\theta_{ij})]\\ &P_{ei} = E'_{qi}I_{qi} + E'_{di}I_{di},\ Q_{ei} = E'_{qi}I_{di} - E'_{di}I_{qi}\end{aligned}, \quad (4)$$

where all symbols carry their usual meanings in power systems that are presented in [17, 32]. The algebraic equations for d- and q-axis currents along with the electrical power are used with the dynamical models and the final model can be represented as:

$$\begin{aligned}\dot{\delta}_i &= \omega_i - \omega_{0i}\\ \dot{\omega}_i &= -\frac{D_i}{2H_i}(\omega_i - \omega_{0i}) + \frac{\omega_{0i}}{2H_i}[P_{mi} - (E'_{qi}I_{qi} + E'_{di}I_{di})]\\ \dot{E}'_{qi} &= -\frac{1}{T'_{doi}}E'_{qi} - \frac{(x_{di}-x'_{di})}{T'_{doi}}I_{di} + \frac{1}{T'_{doi}}E_{fdi}\\ \dot{E}'_{di} &= -\frac{1}{T'_{qoi}}E'_{di} + \frac{(x_{qi}-x'_{qi})}{T'_{qoi}}I_{qi}\\ \dot{E}_{fdi} &= -\frac{E_{fdi}}{T_{Ai}} + \frac{K_{Ai}}{T_{Ai}}(\Delta V_i + V_{ci})\end{aligned}. \quad (5)$$

The excitation control problem can be formulated using this dynamical model by considering variations in parameters. The parameter dependency of the EABEC can be determined by looking at the response of a particular generator while varying parameters from their nominal values. The parameters which severely affect the stability can be incorporated as unknown in Equation (5). The following section discusses the effects of such variations through the speed deviation response of a generator and the control problem is formulated accordingly and then adaptation laws are used for adapting all these parameters.

3 | FORMULATION OF THE EXCITATION CONTROL PROBLEM

Parameters of different components appear in the final dynamical model in Equation (5). Since excitation controllers are generally implemented locally, these excitation control law should include for parameters related to transmission lines that connect different buses [16]. However, the implementation of excitation controllers cannot avoid parameters associated with synchronous generators and excitation systems for tackling transient behaviors due to large disturbances. As a result, the performance of such controllers is heavily reliant on the parametric information and other feedback variables (e.g. voltage, current, active power, reactive power, speed etc.) that can be obtained from measurements. At the same time, it is hard to use the proper values of parameters as many of these such as transient parameters (e.g. T'_{doi} and T'_{qoi}) change when power systems experience disturbances.

The impacts of changes in parameter on an EABEC are investigated in terms of managing the stable operation by applying this EABEC an IEEE test system having 10 synchronous generator and 39 buses as shown in Figure 4 in which different parameters of generators and exciters are varied from their nominal values. The speed deviation of G4 at bus-33, is monitored to analyze these effects. Here, the main objective of Figure 1 is to present the effects of parameter sensitivity on the speed deviation of G4 with variations of different parameters appearing in the dynamical mode as represented by Equation (5). The speed deviation of G4 is maintained at zero as shown in Figure 1 when the proper values (commonly known as the nominal values) of parameters are used which is mainly due to no changes in parameters. This clearly demonstrates the operation of G4 at the synchronous speed. However, this operating scenario is disturbed by changing parameters from their nominal values where these changes are basically 10% from their nominal values. The following sequences are considered to change the values of parameters:

- change of D_i;
- change of D_i and H_i;
- change of D_i, H_i, and T'_{doi};
- change of D_i, H_i, T'_{doi}, and T'_{qoi}; and
- change of D_i, H_i, T'_{doi}, T'_{qoi} and T_{Ai}.

In all cases, the speed deviation response of G4 is disturbed due to variations in parameters. If all these parameters in Equation (5) are considered as unknown, it can be written as:

$$\theta_{1i} = -\frac{D_i}{2H_i},\ \theta_{2i} = \frac{\omega_{0i}}{2H_i}, \theta_{3i} = \frac{1}{T'_{doi}},\ \theta_{4i} = -\frac{(x_{di} - x'_{di})}{T'_{doi}},$$
$$\theta_{5i} = -\frac{1}{T'_{qoi}},\ \theta_{6i} = \frac{x_{qi} - x'_{qi}}{T'_{qoi}},\ \theta_{7i} = -\frac{1}{T_{Ai}},\ \theta_{8i} = \frac{K_{Ai}}{T_{Ai}} \quad . (6)$$

It is worth to mention that the variations in parameters are considered as global instead of restricting within a range as discussed in [22]. It is also worth noting that these parameters will be adapted by sensing the transient characteristics.

The proposed ABEC will provide robust operation when power systems experience severe transients that cause significant variations in parameters. This will be possible if the dynamical model is represented in terms of unknown parameters and these parameters estimated using adaptation laws. The incorporation of these unknown parameters will simplify Equation (5) as:

$$\begin{aligned}
\dot{x}_{1i} &= x_{2i} \\
\dot{x}_{2i} &= \theta_{1i}x_{2i} + \theta_{2i}(P_{mi} - I_{qi}x_{3i} - I_{di}x_{4i}) \\
\dot{x}_{3i} &= -\theta_{3i}x_{3i} + \theta_{4i}I_{di} + \theta_{3i}x_{5i} \\
\dot{x}_{4i} &= \theta_{5i}x_{4i} + \theta_{6i}I_{qi} \\
\dot{x}_{5i} &= \theta_{7i}x_{5i} + \theta_{8i}(\Delta V_i + V_{ci})
\end{aligned} \quad , \quad (7)$$

where $x_{1i}, x_{2i}, x_{3i}, x_{4i}$, and x_{5i} represent δ_i, $\omega_i - \omega_{0i}$, E'_{qi}, E'_{di}, and E_{fdi}, respectively. The excitation control and parameter adaptation laws derived from this model will ensure the augmentation of the transient stability where these derivations are discussed in the section below.

4 | PROPOSED ADAPTIVE EXCITATION CONTROL SCHEME

A step-by-step process is presented in this section to derive the excitation control and parameter adaptation laws using the proposed scheme. Each step analyzes the stability of relevant error dynamics for both states and unknown parameter while the relationship among different states is presented by introducing virtual control law to ensure intermediate stability until the final excitation control and parameter adaptation laws are achieved. Adaptation laws estimate all parameters that are assumed as unknown and the excitation control law uses these estimated values for ensuring the stability during large faults and robustness against variations in parameters which are discussed in the following steps.

Step 1: The controller design process needs to start with analyzing the stability of the tracking error (e_{1i}) for the first state, that is, the rotor angle finally represented as x_{1i}. If x_{1di} corresponds the desired value of x_{1i}, e_{1i} can be written as:

$$e_{1i} = x_{1i} - x_{1di}, \quad (8)$$

and its dynamic will be as:

$$\dot{e}_{1i} = \dot{x}_{1i} = x_{2i}. \quad (9)$$

As the excitation control input and unknown parameters do not appear in (9), the next state (x_{2i}) can be treated as a virtual control input for stabilizing $\dot{e}_{1i}$ where it actually corresponds to the speed deviation, that is, $\dot{e}_{1i} = x_{2i}$. The CLF for analyzing the convergence of e_{1i} can be formulated as:

$$W_{1i} = \frac{1}{2}e_{1i}^2, \quad (10)$$

and the simplified form of its derivative as:

$$\dot{W}_{1i} = e_{1i}x_{2i}. \quad (11)$$

The convergence of e_{1i} depends on the values of $\dot{W}_{1i}$ and it will converge if $\dot{W}_{1i} \leq 0$ (i.e. negative semi-definite) or $\dot{W}_{1i} < 0$ (i.e. negative definite). If β_i, a new control variable with $\beta_i \approx x_{2i}$ assists to ensure $\dot{W}_{1i} \leq 0$; β_i has to be a feedback controller of the following form for minimizing e_{1i}:

$$\beta_i = -k_{1i}e_{1i}, \quad (12)$$

where k_{1i} represents a user-defined positive value that controls the convergence speed of e_{1i}. Using $\beta_i = -k_{1i}e_{1i}$ in Equation (13), the stability of $\dot{e}_{1i}$ can be ensured as the following condition holds:

$$\dot{W}_{1i} = -k_{1i}e_{1i}^2, \quad (13)$$

which indicates $\dot{W}_{1i} \leq 0$ for any values of e_{1i} and thereby, guaranteeing $e_{1i} \to 0$. To further proceed with the design process, β_i needs to be used as a reference value of x_{2i} and since $\dot{e}_{1i} = x_{2i}$, $\dot{\beta}_i$ can be obtained as:

$$\dot{\beta}_i = -k_{1i}x_{2i}. \quad (14)$$

Step 2: Since β_i is the reference value of x_{2i} , e_{2i} can be defined as:

$$e_{2i} = x_{2i} - \beta_i, \quad (15)$$

and $\dot{e}_{2i}$ will be as:

$$\dot{e}_{2i} = \theta_{1i}x_{2i} + \theta_{2i}(P_{mi} - I_{qi}x_{3i} - I_{di}x_{4i}) + k_{1i}x_{2i}. \quad (16)$$

If $\tilde{\theta}_{1i}$ and $\tilde{\theta}_{2i}$ represent the parameter estimation errors with $\hat{\theta}_{1i}$ and $\hat{\theta}_{2i}$ as estimated values corresponding to parameters θ_{1i} and θ_{2i}, respectively; these can be expressed as:

$$\tilde{\theta}_{1i} = \theta_{1i} - \hat{\theta}_{1i} \text{ and } \tilde{\theta}_{2i} \quad = \theta_{2i} - \hat{\theta}_{2i}. \quad (17)$$

With these, Equation (16) can be rewritten as:

$$\begin{aligned}\dot{e}_{2i} = {} & (\hat{\theta}_{1i} + \tilde{\theta}_{1i})x_{2i} + (\hat{\theta}_{2i} \\ & + \tilde{\theta}_{2i})(P_{mi} - I_{qi}x_{3i} - I_{di}x_{4i}) + k_{1i}x_{2i}.\end{aligned} \quad (18)$$

The convergence of e_{2i} can be analyzed through the following CLF:

$$W_{2i} = W_{1i} + \frac{1}{2}e_{2i}^2, \quad (19)$$

and its derivative will be as:

$$\begin{aligned}\dot{W}_{2i} = {} & -k_{1i}e_{1i}^2 + e_{2i}[(\hat{\theta}_{1i} + \tilde{\theta}_{1i})x_{2i} + (\hat{\theta}_{2i} + \tilde{\theta}_{2i}) \\ & (P_{mi} - I_{qi}x_{3i} - I_{di}x_{4i}) + k_{1i}x_{2i}],\end{aligned} \quad (20)$$

which can be rewritten as:

$$\begin{aligned}\dot{W}_{2i} = {} & -k_{1i}e_{1i}^2 + e_{2i}[\hat{\theta}_{1i}x_{2i} + \hat{\theta}_{2i}(P_{mi} - I_{qi}x_{3i} - I_{di}x_{4i}) \\ & + k_{1i}x_{2i}] - \frac{1}{\gamma_{1i}}\tilde{\theta}_{1i}(\dot{\hat{\theta}}_{1i} - \gamma_{1i}e_{2i}x_{2i}) - \\ & \frac{1}{\gamma_{2i}}\tilde{\theta}_{2i}[\dot{\hat{\theta}}_{2i} - \gamma_{2i}e_{2i}(P_{mi} - I_{qi}x_{3i} - I_{di}x_{4i})],\end{aligned} \quad (21)$$

where γ_{1i} and γ_{2i} are positive adaption gains that are used for controlling the convergence speed of $\tilde{\theta}_{1i}$ and $\tilde{\theta}_{2i}$, respectively.

Since the excitation control input and remaining unknown parameters are not yet appeared, the remaining states (e.g. x_{3i} and x_{4i}) can be used as virtual control inputs to demonstrate their relationship with previous states. To achieve $\dot{W}_{2i} \leq 0$, the new forms of controllers (i.e. $\beta_{1i} \approx x_{3i}$ and $\beta_{2i} \approx x_{4i}$) can be obtained as:

$$\begin{aligned}\beta_{1i} &= \frac{1}{\hat{\theta}_{2i}I_{qi}}(\hat{\theta}_{1i}x_{2i} + \hat{\theta}_{2i}P_{mi} + k_{1i}x_{2i}) \\ \beta_{2i} &= \frac{1}{\hat{\theta}_{2i}I_{di}}k_{2i}e_{2i}\end{aligned}, \quad (22)$$

where k_{2i} represents a user-defined positive value that controls the convergence speed of e_{2i}. At this stage, parameter adaptation laws are not decided for estimating unknown parameters θ_{1i} and θ_{2i} as the excitation control law is not obtained yet and there will be over- or under-parameterization problems if these are estimated now. However, it is essential to ensure the stability with the virtual variables β_{1i} and β_{2i} for which the following tuning functions are defined:

$$\tau_{1i} = \gamma_{1i}e_{2i}x_{2i} \text{ and } \tau_{2i} = \gamma_{2i}e_{2i}(P_{mi} - I_{qi}x_{3i} - I_{di}x_{4i}). \quad (23)$$

With these (i.e. Equations (22) and (23)), the simplified form of Equation (21) will be:

$$\begin{aligned}\dot{W}_{2i} = {} & -\sum_{j=1}^{2} k_{ji}e_{ji}^2 - \frac{1}{\gamma_{1i}}\tilde{\theta}_{1i}(\dot{\hat{\theta}}_{1i} - \tau_{1i}) \\ & - \frac{1}{\gamma_{2i}}\tilde{\theta}_{2i}(\dot{\hat{\theta}}_{2i} - \tau_{2i}).\end{aligned} \quad (24)$$

The first term in Equation (24) will be negative semi-definite for any values of e_{1i} and e_{2i} while the last two terms will be the same if $\dot{\hat{\theta}}_{1i} \leq \tau_{1i}$ and $\dot{\hat{\theta}}_{2i} \leq \tau_{2i}$. However, the last two terms are associated with θ_{2i} and θ_{2i} and no decisions are made for these estimations. The estimation problems for these parameters will be sorted out during the final stage when the excitation control input will be determined. Hence, it is essential to analyze the characteristics of other steps as discussed below.

Step 3: Since $\beta_{1i} \approx x_{3i}$ and $\beta_{2i} \approx x_{4i}$, the corresponding errors (i.e. e_{3i} and e_{4i}) will be as:

$$e_{3i} = x_{3i} - \beta_{1i} \text{ and } e_{4i} = x_{4i} - \beta_{2i}. \quad (25)$$

The derivative of e_{3i}, by incorporating the third equation in (7) can be written as:

$$\begin{aligned}\dot{e}_{3i} = {} & \theta_{4i}I_{di} - \theta_{3i}x_{3i} + \theta_{3i}x_{5i} - T_{1i} \\ & + T_{2i} - T_{4i}\theta_{1i} - T_{5i}\theta_{2i},\end{aligned} \quad (26)$$

with

$$\dot{\beta}_{1i} = T_{1i} - T_{2i} + T_{4i}\theta_{1i} + T_{5i}\theta_{2i}, \quad (27)$$

where

$$\begin{aligned}T_{1i} &= \frac{\dot{\hat{\theta}}_{2i}P_{mi} + \hat{\theta}_{2i}\dot{P}_{mi} + x_{2i}\dot{\hat{\theta}}_{1i}}{\hat{\theta}_{2i}I_{qi}}, \\ T_{2i} &= \frac{(\dot{\hat{\theta}}_{2i}I_{qi} + \hat{\theta}_{2i}\dot{I}_{qi})[\hat{\theta}_{2i}P_{mi} + x_{2i}T_{3i}]}{\hat{\theta}_{2i}^2I_{qi}^2},\end{aligned} \quad (28)$$

$T_{3i} = \hat{\theta}_{1i} + k_{1i}$, $T_{4i} = T_{3i}x_{2i}$, and

$T_{5i} = T_{3i}(P_{mi} - I_{qi}x_{3i} - I_{di}x_{4i})$.

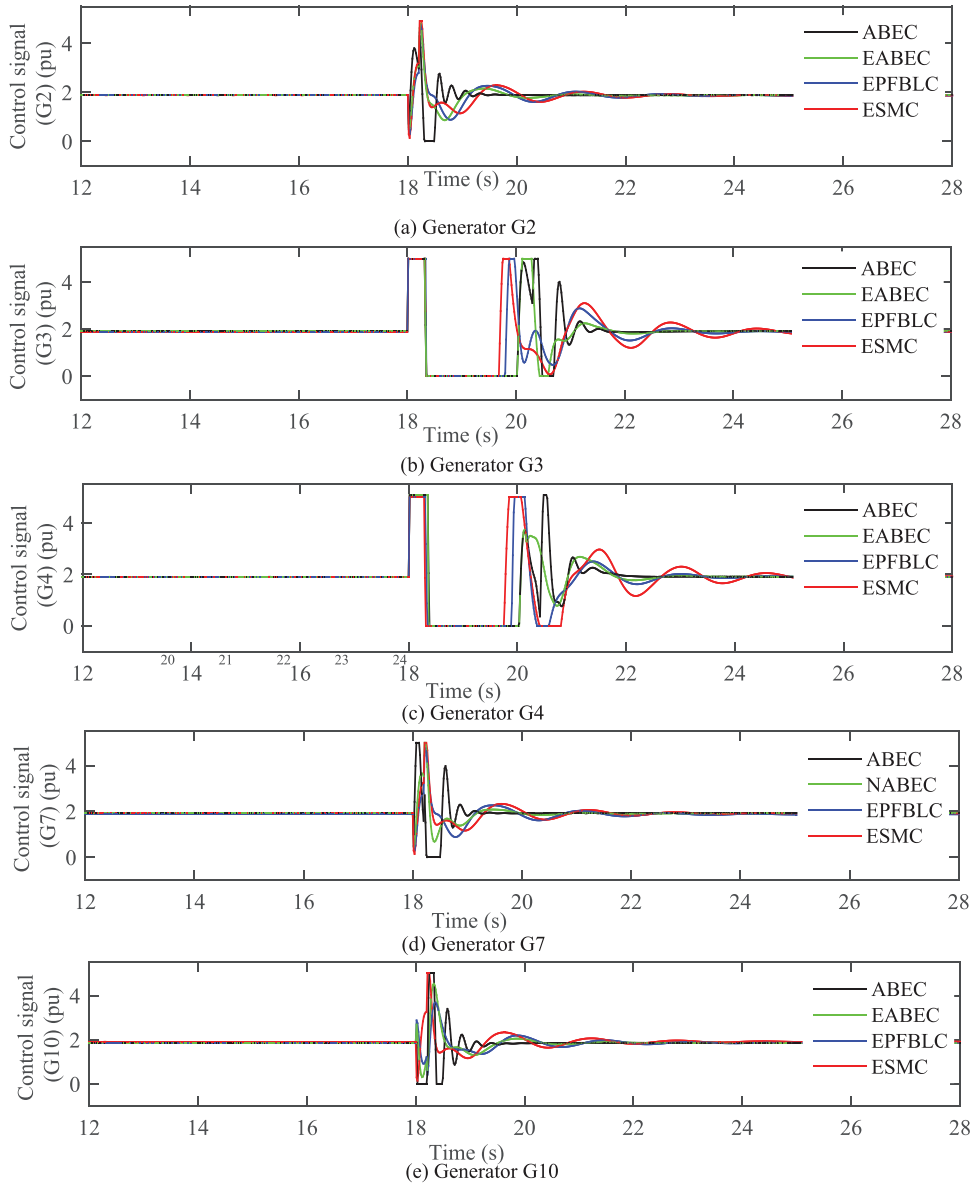

FIGURE 9 Control signals with a symmetrical 3LG fault at the terminal of G4

If $\tilde{\theta}_{3i} = \theta_{3i} - \hat{\theta}_{3i}$ and $\tilde{\theta}_{4i} = \theta_{4i} - \hat{\theta}_{4i}$ are corresponding parameter estimation errors for θ_{3i} and θ_{4i} with their estimated values of $\hat{\theta}_{4i}$ and $\hat{\theta}_{4i}$, respectively; the substitutions of these values into Equation (26) yield:

$$\dot{e}_{3i} = -(\hat{\theta}_{3i} + \tilde{\theta}_{3i})(x_{3i} - x_{5i}) + (\hat{\theta}_{4i} + \tilde{\theta}_{4i})I_{di} - T_{1i} + T_{2i} - T_{4i}(\hat{\theta}_{1i} + \tilde{\theta}_{1i}) - T_{5i}(\hat{\theta}_{2i} + \tilde{\theta}_{2i}). \tag{29}$$

The same approach will yield the dynamic of e_{4i} as:

$$\dot{e}_{4i} = (\hat{\theta}_{5i} + \tilde{\theta}_{5i})x_{4i} + (\hat{\theta}_{6i} + \tilde{\theta}_{6i})I_{qi} - \dot{\beta}_{2i}, \tag{30}$$

where $\hat{\theta}_{5i}$ and $\hat{\theta}_{6i}$ are the estimated values of θ_{5i} and θ_{6i}, respectively; and the estimation errors for θ_{5i} and θ_{6i} are expressed as $\tilde{\theta}_{5i} = \theta_{5i} - \hat{\theta}_{5i}$ and $\tilde{\theta}_{6i} = \theta_{6i} - \hat{\theta}_{6i}$, respectively. The CLF for analyzing the convergence of e_{1i} to e_{4i} can be formulated as:

$$W_{3i} = W_{2i} + \frac{1}{2}(e_{3i}^2 + e_{4i}^2 + \frac{1}{\gamma_{3i}}\tilde{\theta}_{3i}^2 + \frac{1}{\gamma_{4i}}\tilde{\theta}_{4i}^2 + \frac{1}{\gamma_{5i}}\tilde{\theta}_{5i}^2 + \frac{1}{\gamma_{6i}}\tilde{\theta}_{6i}^2), \tag{31}$$

where γ_{3i}, γ_{4i}, γ_{5i}, and γ_{6i} are positive adaptation gains. For analyzing the stability of $\dot{e}_{1i}$ to $\dot{e}_{4i}$ and convergence of $\tilde{\theta}_{1i}$ to $\tilde{\theta}_{6i}$,

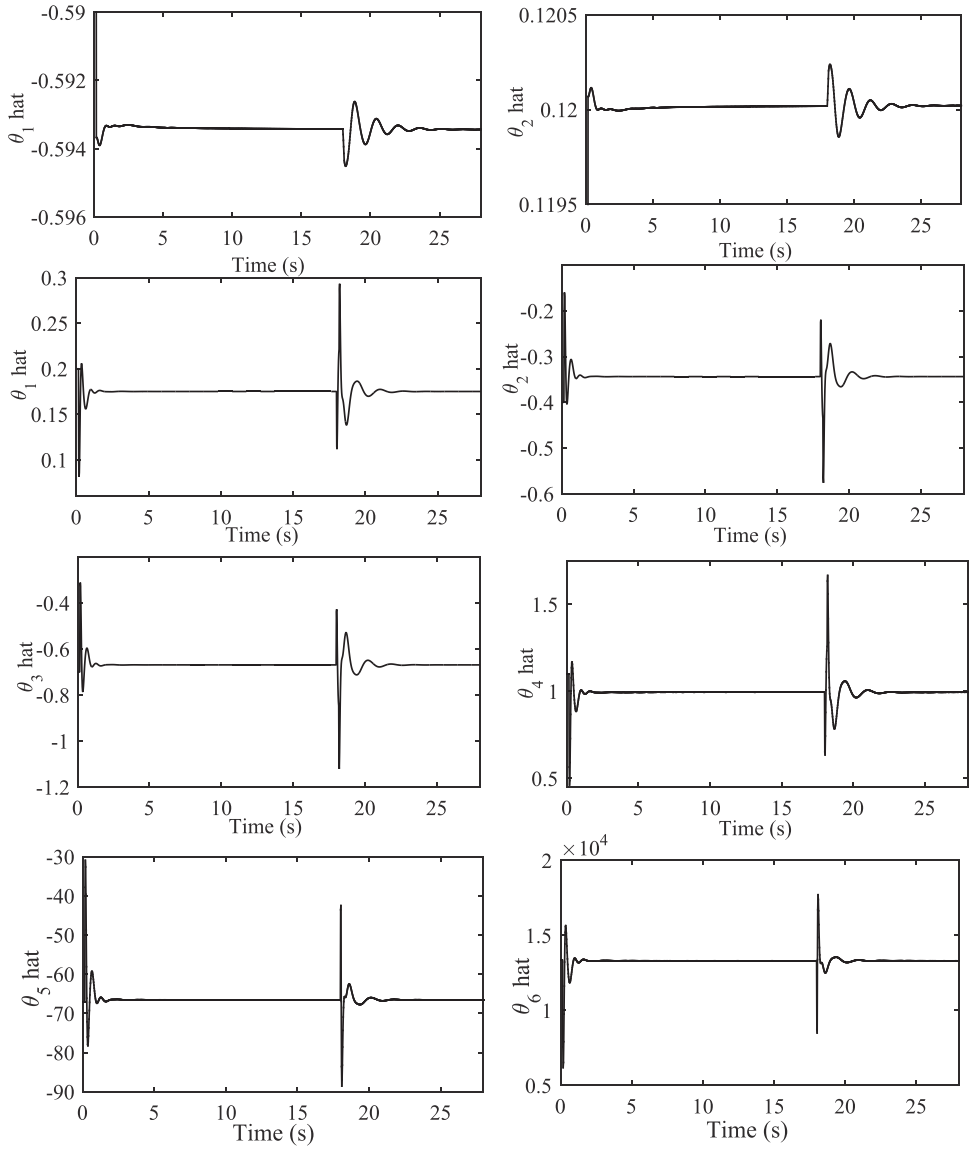

FIGURE 10 Estimated unknown parameters of G4 with a symmetrical 3LG fault at the terminal of G4

$\dot{W}_{3i}$ can be determined as:

$$\begin{aligned}\dot{W}_{3i} = &-\sum_{j=1}^{2} k_{ji} e_{ji}^2 + e_{3i}[\hat{\theta}_{4i} I_{di} - \hat{\theta}_{3i}(x_{3i} - x_{5i}) \\ &- T_{1i} + T_{2i} - T_{4i}\hat{\theta}_{1i} - T_{5i}\hat{\theta}_{2i}] + e_{4i}(\hat{\theta}_{5i} x_{4i} + \hat{\theta}_{6i} \\ &- \dot{\beta}_{2i}) - \frac{1}{\gamma_{1i}}\tilde{\theta}_{1i}(\dot{\hat{\theta}}_{1i} - \tau_{1i} + \gamma_{1i} e_{3i} T_{4i}) - \frac{1}{\gamma_{2i}}\tilde{\theta}_{2i} \\ &(\dot{\hat{\theta}}_{2i} - \tau_{2i} + \gamma_{2i} e_{3i} T_{5i}) - \frac{1}{\gamma_{3i}}\tilde{\theta}_{3i}[\dot{\hat{\theta}}_{3i} + \gamma_{3i} e_{3i} \\ &(x_{3i} - x_{5i})] - \frac{1}{\gamma_{4i}}\tilde{\theta}_{4i}(\dot{\hat{\theta}}_{4i} - \gamma_{4i} e_{4i} I_{di}) \\ &- \frac{1}{\gamma_{5i}}\tilde{\theta}_{5i}(\dot{\hat{\theta}}_{5i} - \gamma_{5i} e_{4i} x_{4i}) - \frac{1}{\gamma_{6i}}\tilde{\theta}_{6i}(\dot{\hat{\theta}}_{6i} - \gamma_{6i} e_{4i} I_{qi}).\end{aligned} \tag{32}$$

A new control variable, $\beta_{3i} \approx x_{5i}$ needs to be determined as follows for ensuring the stability of $\dot{e}_{3i}$ and $\dot{e}_{4i}$:

$$\begin{aligned}\beta_{3i} = &\frac{1}{\hat{\theta}_{3i}}[\hat{\theta}_{4i} I_{di} - \hat{\theta}_{3i} x_{3i} - T_{1i} + T_{2i} \\ &- T_{4i}\hat{\theta}_{1i} - T_{5i}\hat{\theta}_{2i} - k_{3i} e_{3i}] \\ &\hat{\theta}_{5i} x_{4i} + \hat{\theta}_{6i} I_{qi} - \dot{\beta}_{2i} = -k_{4i} e_{4i},\end{aligned} \tag{33}$$

where k_{3i} and k_{4i} represent user-defined positive values that control the convergence speed of e_{3i} and e_{4i}, respectively. As there are still two unknown parameters θ_{7i} and θ_{8i} which are not appeared yet during the analysis, the values of $\theta_{1i}, \theta_{2i}, \theta_{3i}, \theta_{4i}, \theta_{5i}$, and θ_{6i} are not estimated in this step for avoiding over-parameterization problems. Despite not updating the values of $\hat{\theta}_{1i}, \hat{\theta}_{2i}, \hat{\theta}_{3i}, \hat{\theta}_{4i}, \hat{\theta}_{5i}$, and $\hat{\theta}_{6i}$; the corresponding tuning functions

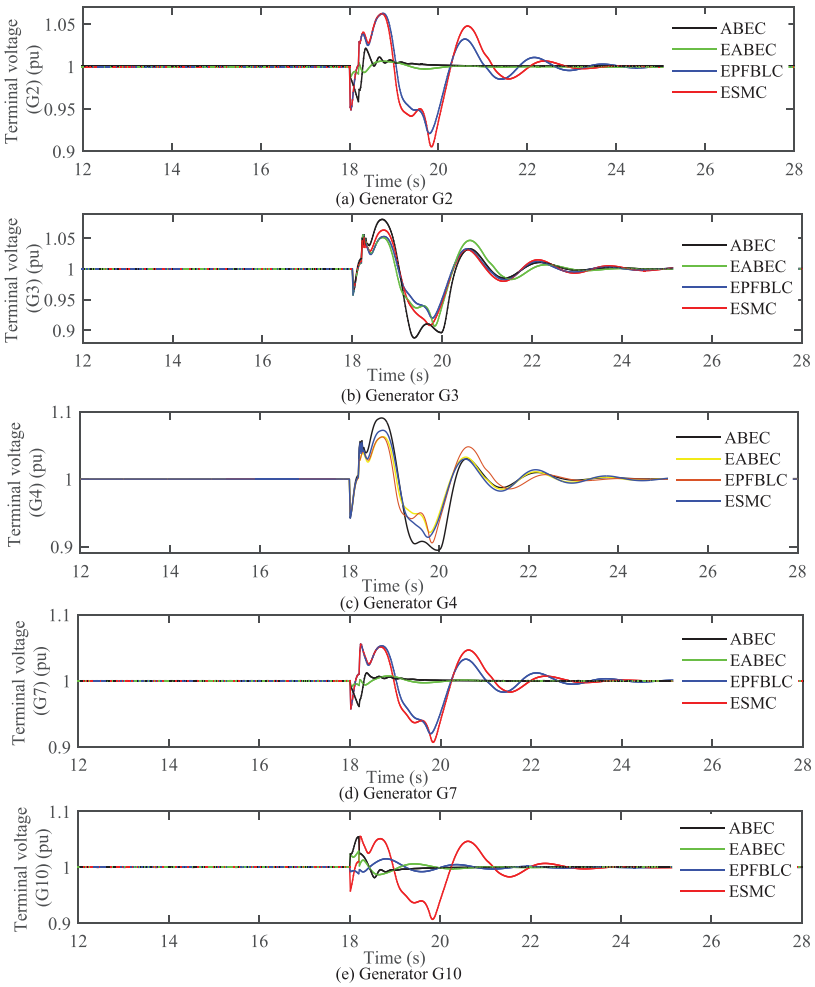

FIGURE 11 Terminal voltages with a symmetrical 3LG fault on the line connecting bus-16 and bus-19

need to be defined as follows for ensuring the stability:

$$\tau_{11i} = \tau_{1i} - \gamma_{1i} e_{3i} T_{4i},\ \tau_{22i} = \tau_{2i} - \gamma_{2i} e_{3i} T_{5i}$$
$$\tau_{3i} = \gamma_{3i} e_{3i} (x_{3i} - x_{5i}),\ \tau_{4i} = \gamma_{4i} e_{3i} I_{di}, \tag{34}$$
$$\tau_{5i} = \gamma_{5i} e_{4i} x_{4i},\ \text{and}\ \tau_{6i} = \gamma_{6i} e_{4i} I_{qi}.$$

The substitutions of Equations (33) and (34) into Equation (32) yield:

$$\dot{W}_{3i} = -\sum_{j=1}^{4} k_{ji} e_{ji}^2 - \frac{1}{\gamma_{1i}} \tilde{\theta}_{1i} (\dot{\hat{\theta}}_{1i} - \tau_{11i}) - \frac{1}{\gamma_{2i}} \tilde{\theta}_{2i} (\dot{\hat{\theta}}_{2i} - \tau_{22i})$$
$$- \frac{1}{\gamma_{3i}} \tilde{\theta}_{3i} (\dot{\hat{\theta}}_{3i} + \tau_{3i}) - \frac{1}{\gamma_{4i}} \tilde{\theta}_{4i} (\dot{\hat{\theta}}_{4i} - \tau_{4i}) \tag{35}$$
$$- \frac{1}{\gamma_{5i}} \tilde{\theta}_{5i} (\dot{\hat{\theta}}_{5i} - \tau_{5i}) - \frac{1}{\gamma_{6i}} \tilde{\theta}_{6i} (\dot{\hat{\theta}}_{6i} - \tau_{6i}).$$

The negative semi-definiteness of $\dot{W}_{3i}$ can be clearly seen from the right side of Equation (31), except the last four terms. The decisions about remaining terms are not made in this step due to the absence of other parameters and excitation control input which will be fixed in the final step. Before moving to the final step, β_{3i} can be obtained as:

$$\dot{\beta}_{3i} = A_i - B_i (x_{3i} - x_{5i}) \theta_{1i} + B_i I_{di} \theta_{2i} + C_{1i}, \tag{36}$$

where

$$A_i = \frac{1}{\hat{\theta}_{1i}} (\ddot{\beta}_{1i} - \dot{\hat{\theta}}_{2i} I_{di} - \dot{I}_{di} \hat{\theta}_{2i} + k_{3i} \dot{\beta}_{1i}) - \frac{\dot{\hat{\theta}}_{1i}}{\hat{\theta}_{1i}^2} (\dot{\beta}_{1i} - \hat{\theta}_{2i} I_{di}$$
$$- k_{3i} e_{3i}),\ B_i = 1 - \frac{k_{3i}}{\hat{\theta}_{1i}},\ \text{and}\ C_{1i} = \dot{T}_{2i} - \dot{T}_{1i} - \dot{T}_{4i} \hat{\theta}_{1i} \tag{37}$$
$$- T_{4i} \dot{\hat{\theta}}_{1i} - \dot{T}_{5i} \hat{\theta}_{2i} - T_{5i} \dot{\hat{\theta}}_{2i} - k_{3i} \dot{e}_{3i}.$$

The next step will be the final step which will present the derivation of parameter adaptation and excitation control laws.

Step 4: As $\beta_{3i} \approx x_{5i}$, the corresponding error (i.e. e_{5i}) can be expressed as:

$$e_{5i} = x_{5i} - \beta_{3i}, \tag{38}$$

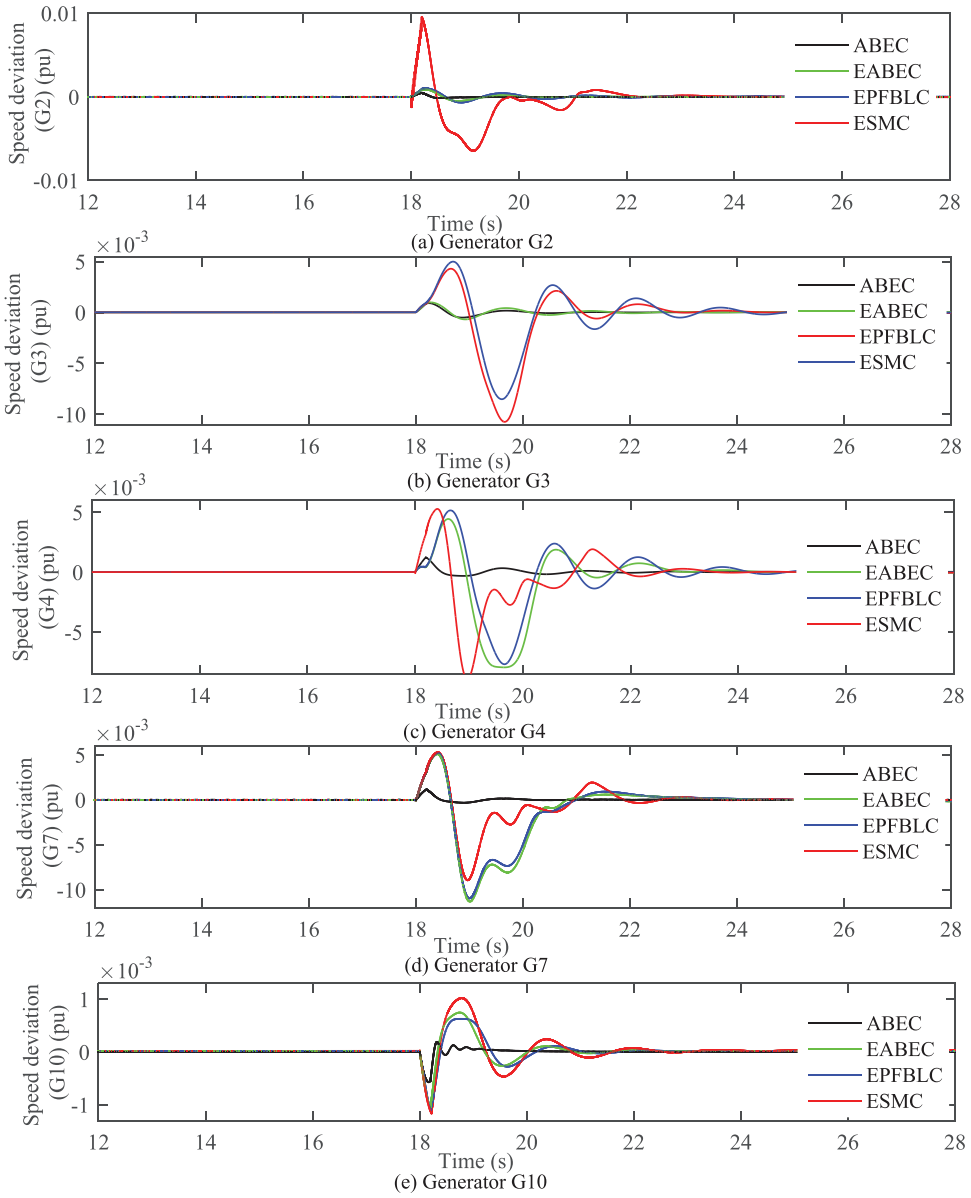

FIGURE 12 Speed deviations with a symmetrical 3LG fault on the line connecting bus-16 and bus-19

and its dynamic as:

$$\begin{aligned}\dot{e}_{5i} =& \theta_{7i}x_{5i} + \theta_{8i}(\Delta V_i + V_{ci}) - A_i + B_i(x_{3i} - x_{5i})\\ & \theta_{1i} - B_i I_{di}\theta_{2i} - C_{1i}.\end{aligned} \tag{39}$$

If $\tilde{\theta}_{7i} = \theta_{7i} - \hat{\theta}_{7i}$ and $\tilde{\theta}_{8i} = \theta_{8i} - \hat{\theta}_{8i}$ are parameter estimation errors for unknown parameters θ_{7i} and θ_{8i} with their estimated values as $\hat{\theta}_{7i}$ and $\hat{\theta}_{8i}$, respectively; Equation (39) will have the following form:

$$\begin{aligned}\dot{e}_{5i} =& (\hat{\theta}_{7i} + \tilde{\theta}_{7i})x_{5i} + (\hat{\theta}_{8i} + \tilde{\theta}_{8i})(\Delta V_i + V_{ci}) - A_i +\\ & B_i(x_{3i} - x_{5i})(\hat{\theta}_{3i} + \tilde{\theta}_{3i}) - B_i I_{di}(\hat{\theta}_{4i} + \tilde{\theta}_{4i}) - C_{1i}.\end{aligned} \tag{40}$$

Equation (40) includes ll stability parameters which need to be estimated and the excitation control input V_{ci}. Hence, it is the time to decide about the parameter estimation and the excitation control laws in a way that $e_{1i} \to 0$, $e_{2i} \to 0$, $e_{3i} \to 0$, $e_{4i} \to 0$, $e_{5i} \to 0$, $\tilde{\theta}_{1i} \to 0$, $\tilde{\theta}_{2i} \to 0$, $\tilde{\theta}_{3i} \to 0$, $\tilde{\theta}_{4i} \to 0$, $\tilde{\theta}_{5i} \to 0$, $\tilde{\theta}_{6i} \to 0$, $\tilde{\theta}_{7i} \to 0$, and $\tilde{\theta}_{8i} \to 0$ as $t \to \infty$ while capturing all nonlinearities in the excitation control input so that it can provide adequate damping into the system for preserving the stability against large disturbances. For analyzing these, the final CLF will be as:

$$W_{4i} = W_{3i} + \frac{1}{2}\left(e_{5i}^2 + \frac{1}{\gamma_{7i}}\tilde{\theta}_{7i}^2 + \frac{1}{\gamma_{8i}}\tilde{\theta}_{8i}^2\right), \tag{41}$$

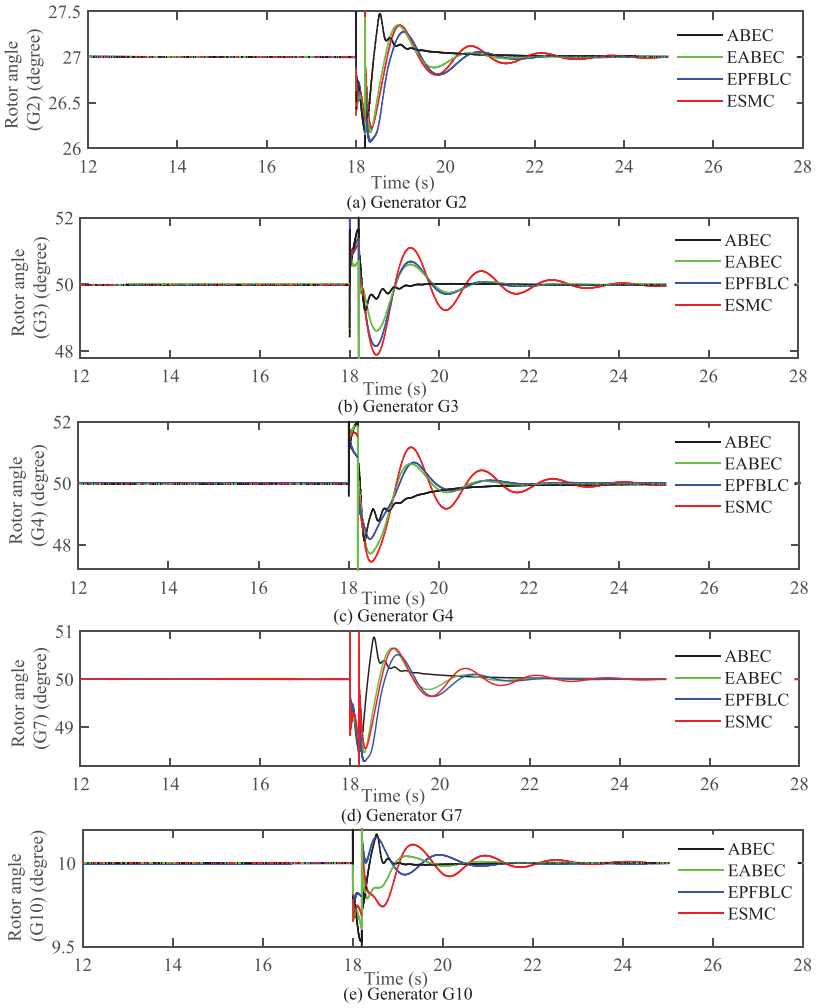

FIGURE 13 Rotor angles with a symmetrical 3LG fault on the line connecting bus-16 and bus-19

and its derivative as:

$$\begin{aligned}\dot{W}_{4i} = &-\sum_{j=1}^{4} k_{ji}e_{ji}^2 + e_{5i}[\hat{\theta}_{7i}x_{5i} \\ &+ \hat{\theta}_{8i}(\Delta V_i + V_{ci})] - A_i + B_i(x_{3i} - x_{5i})\hat{\theta}_{3i} - \hat{\theta}_{4i}B_i \\ &I_{di} - C_{1i}] - \frac{1}{\gamma_{1i}}\tilde{\theta}_{1i}(\dot{\hat{\theta}}_{1i} - \tau_{11i}) - \frac{1}{\gamma_{2i}}\tilde{\theta}_{2i}(\dot{\hat{\theta}}_{2i} - \tau_{22i}) \\ &- \frac{1}{\gamma_{3i}}\tilde{\theta}_{3i}[\dot{\hat{\theta}}_{3i} + \tau_{3i} - \gamma_{3i}e_{5i}B_i(x_{3i} - x_{5i})] - \frac{1}{\gamma_{4i}} \\ &\tilde{\theta}_{4i}(\dot{\hat{\theta}}_{4i} - \tau_{4i} + \gamma_{4i}e_{5i}B_iI_{di}) - \frac{1}{\gamma_{5i}}\tilde{\theta}_{5i}(\dot{\hat{\theta}}_{5i} - \tau_{5i}) \\ &- \frac{1}{\gamma_{5i}}\tilde{\theta}_{4i}(\dot{\hat{\theta}}_{6i} - \tau_{6i}) - \frac{1}{\gamma_{7i}}\tilde{\theta}_{7i}(\dot{\hat{\theta}}_{7i} - \gamma_{7i}e_{5i}x_{5i}) \\ &- \frac{1}{\gamma_{8i}}\tilde{\theta}_{8i}[\dot{\hat{\theta}}_{8i} - \gamma_{8i}e_{5i}(\Delta V_i + V_{ci})].\end{aligned} \tag{42}$$

The following adaptation laws will eliminate the effects of $\tilde{\theta}_{1i}, \tilde{\theta}_{2i}, \tilde{\theta}_{3i}, \tilde{\theta}_{4i}, \tilde{\theta}_{5i}, \tilde{\theta}_{6i}, \tilde{\theta}_{7i}$ and $\tilde{\theta}_{8i}$ in Equation (42):

$$\begin{aligned}&\dot{\hat{\theta}}_{1i} = \tau_{11i},\ \dot{\hat{\theta}}_{2i} = \tau_{22i} \\ &\dot{\hat{\theta}}_{3i} = -\tau_{3i} + \gamma_{3i}e_{5i}B_i(x_{3i} - x_{5i}) \\ &\dot{\hat{\theta}}_{4i} = \tau_{4i} - \gamma_{4i}e_{5i}B_iI_{di} \\ &\dot{\hat{\theta}}_{5i} = \tau_{5i},\ \dot{\hat{\theta}}_{6i} = \tau_{6i},\ \dot{\hat{\theta}}_{7i} = \gamma_{7i}e_{5i}x_{5i} \\ &\dot{\hat{\theta}}_{8i} = \gamma_{8i}e_{5i}(\Delta V_i + V_{ci})\end{aligned} \tag{43}$$

The adaptation laws in Equation (42) will simplify Equation (42) as:

$$\begin{aligned}\dot{W}_{4i} = &-\sum_{j=1}^{4} k_{ji}e_{ji}^2 + e_{5i}[\hat{\theta}_{5i}x_{5i} - C_{1i} + \hat{\theta}_{6i}(\Delta V_i + V_{ci})] \\ &- A_i + B_i(x_{3i} - x_{5i})\hat{\theta}_{1i} - \hat{\theta}_{2i}B_iI_{di}].\end{aligned} \tag{44}$$

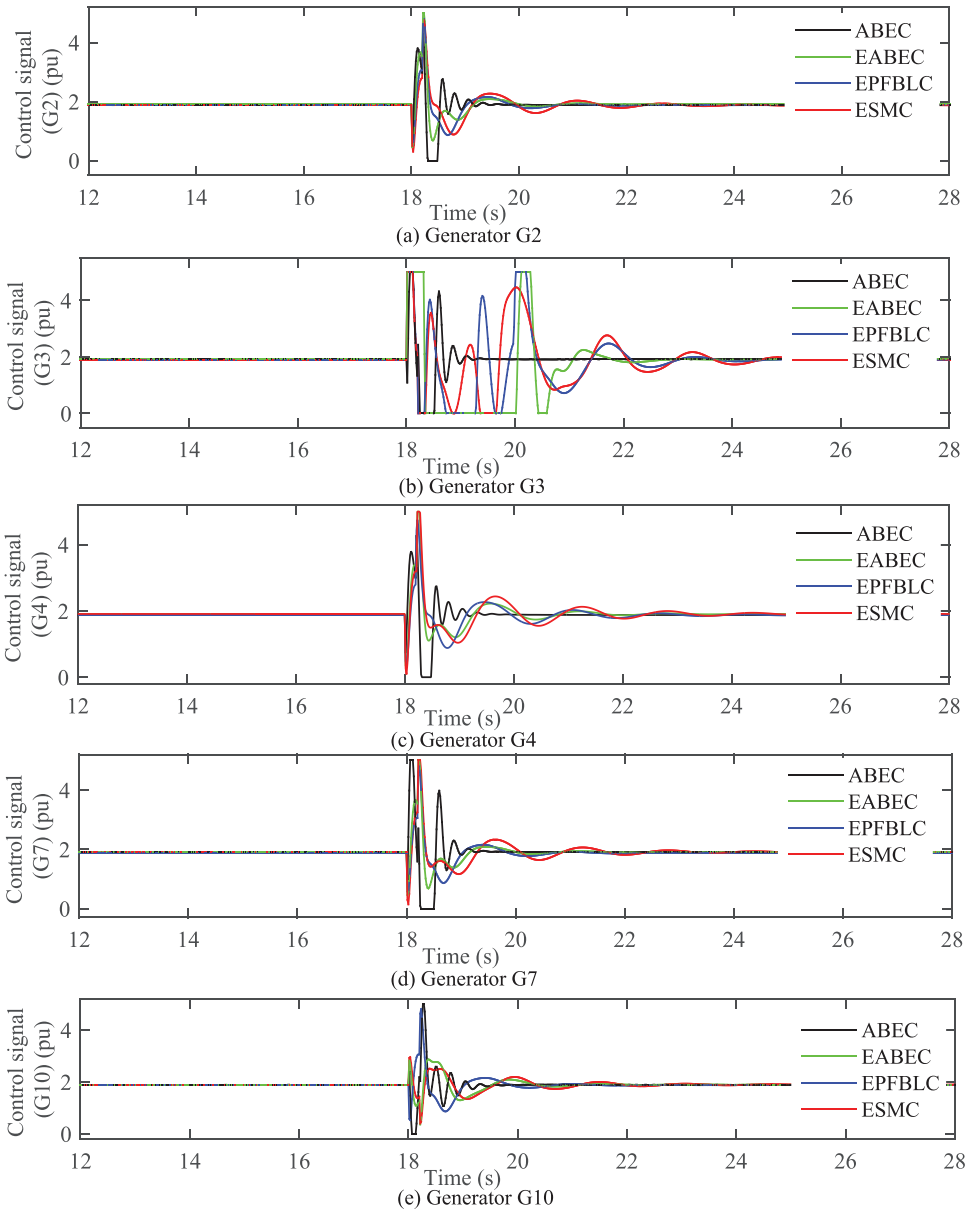

FIGURE 14 Control signals with a symmetrical 3LG fault on the line connecting bus-16 and bus-19

The following excitation control law, that is, V_{ci} will ensure the convergence of all errors:

$$V_{ci} = -\frac{1}{\hat{\theta}_{6i}}[\hat{\theta}_{6i}\Delta V_i + \hat{\theta}_{5i}x_{5i} - A_i + B_i(x_{3i} - x_{5i})\hat{\theta}_{1i} - \hat{\theta}_{2i}B_iI_{di} - C_{1i} + k_{5i}e_{5i}]. \quad (45)$$

This is the final control law and the values of $\hat{\theta}_{1i}$ to $\hat{\theta}_{8i}$ can be obtained from the set of equations in (43). The expressions for A_i, B_i, and C_{1i} are listed in Table 1.

The value of V_{ci} in Equation (45) will simplify Equation (44) as:

$$\dot{W}_{5i} = -k_{1i}e_{1i}^2 - k_{2i}e_{2i}^2 - k_{3i}e_{3i}^2 - k_{4i}e_{4i}^2 - k_{5i}e_{5i}^2 \leq 0 \quad (46)$$

TABLE 1 Expressions for A_i, B_i, and C_{1i} in the control law

$A_i = \frac{1}{\hat{\theta}_{1i}}(\ddot{\beta}_{1i} - \dot{\hat{\theta}}_{2i}I_{di} - \dot{I}_{di}\hat{\theta}_{2i} + k_{3i}\dot{\beta}_{1i}) - \frac{\dot{\hat{\theta}}_{1i}}{\hat{\theta}_{1i}^2}(\dot{\beta}_{1i} - \hat{\theta}_{2i}I_{di} - k_{3i}e_{3i})$, $B_i = 1 - \frac{k_{3i}}{\hat{\theta}_{1i}}$, and $C_{1i} = \dot{T}_{2i} - \dot{T}_{1i} - \dot{T}_{4i}\hat{\theta}_{1i} - T_{4i}\dot{\hat{\theta}}_{1i} - \dot{T}_{5i}\hat{\theta}_{2i} - T_{5i}\dot{\hat{\theta}}_{2i} - k_{3i}\dot{e}_{3i}$

which clearly indicates the condition for ensuring the stability with the newly derived adaptation and excitation control laws. The proposed control is actually a generalized one and it can be employed on any nonlinear models of synchronous generators. For example, it has already been implemented in [22] on synchronous generators represented by the third-order model. The proposed controller requires the measurement of state variables and all these states can be obtained from the algebraic

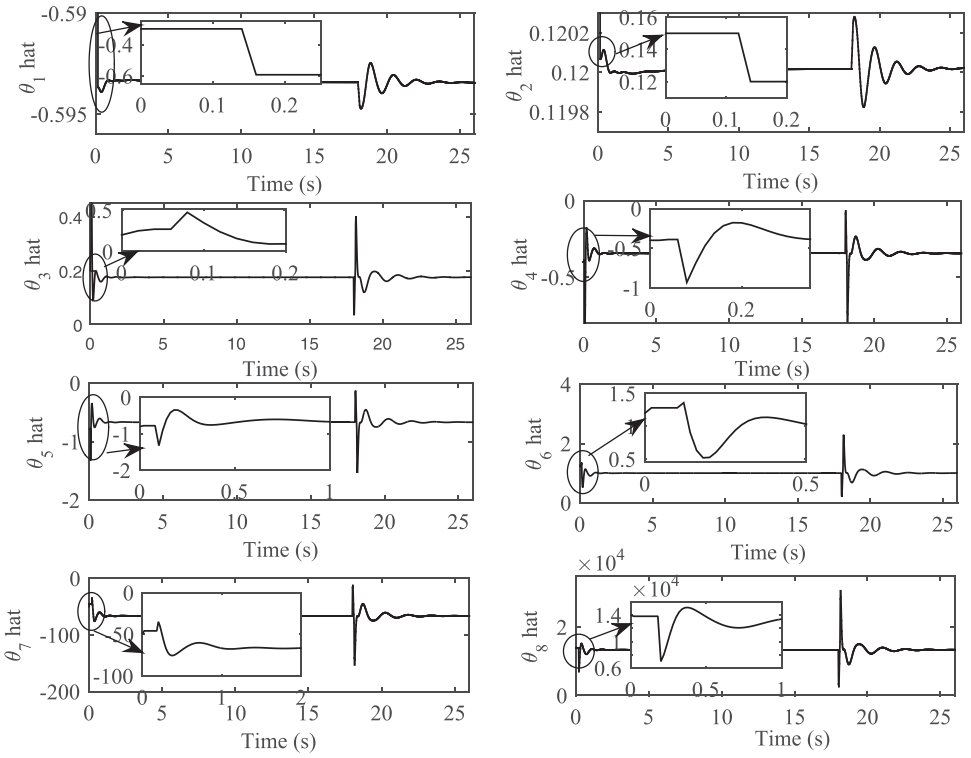

FIGURE 15 Estimated unknown parameters of G4 with a symmetrical 3LG fault on the line connecting bus-16 and bus-19

equations, that is, the steady-state model of power systems. To clearly present the proposed control scheme, a flowchart highlighting each step is presented in Figure 2. At the same time, the implementation block diagram of the proposed ABEC is shown in Figure 3 which includes the key equations (e.g. the system equation as represented by (7) and the control equation in (45)) and the feedback variables. From Figure 3, it can be found that all feedback variables are measured variables which clearly justify the feasibility of the proposed ABEC. It is worth mentioning that the variables appearing in the control signal (45) are internally converted into variables that can directly be measured in order to make the controller applicable to the practical system. Also, all calculations appeared in this section can be done offline and the final control and parameter adaptation laws can be used achieve the desired control objectives. The following section presents simulation results with the proposed scheme under different conditions.

5 | CONTROLLER PERFORMANCE EVALUATION

A large test power system is considered here for evaluating the performance of the designed ABEC over a range of operating conditions. The most commonly used model for evaluating the performance of such a newly designed controller for enhancing the stability, is an IEEE test system having 39 buses and 10 synchronous generators as depicted in Figure 4. The MATLAB/SIMULINK SimPowerSystem Toolbox is used for simulating the test system with the ABEC where several user-defined *S*-function blocks are developed adaptation and excitation control laws. The total power generation in this test power system is 6193.41 MW while having the net demand as 6150.5 MW. This is an interconnected system with 10 synchronous generators (G1 to G10) where transformers and transmission lines are used for interconnecting generators and loads through different buses. One of these 10 synchronous generator, that is, the first synchronous generator (G1) is used as an infinite bus during the simulation and represented through the classical model (GENCLS). The remaining 9 synchronous generators are represented with the two-axis models whose excitation systems are considered as the commonly used IEEE Type II exciters. The simulation model is developed based on all parameters used in [33].

As there are high chances that the excitation voltage may exceed its rated voltage during large disturbances, limiters are used to limit this voltage. In this work, the excitation voltages for each synchronous generator are limited from 0 to 5 pu in order to protect the excitation coil from the overvoltage problem. The designed ABEC can be implemented on all synchronous generators as the excitation control law is obtained in a decentralized manner where this control law is the function of parameters and physical properties of the local generator. However, the application of the designed ABEC to all synchronous generators is not a cost-effective solution as the similar performance can be guaranteed by applying designed ABECs only to those synchronous generators that are vulnerable to large disturbances, that is, changes in operating scenarios due to

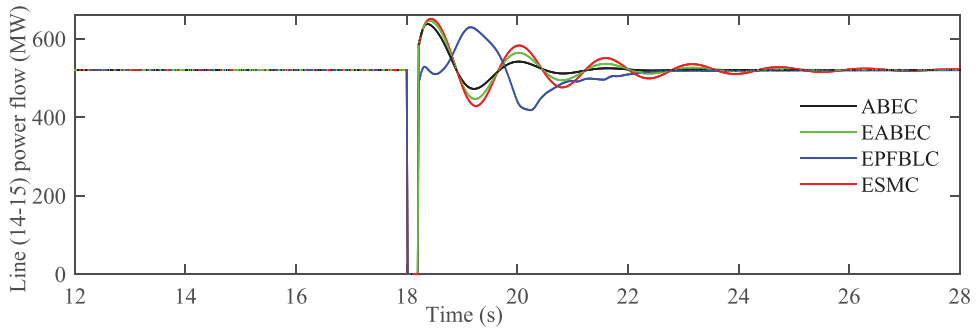

FIGURE 16 Active power flowing through the line connecting bus-15 and bus-16 with the temporary disconnection

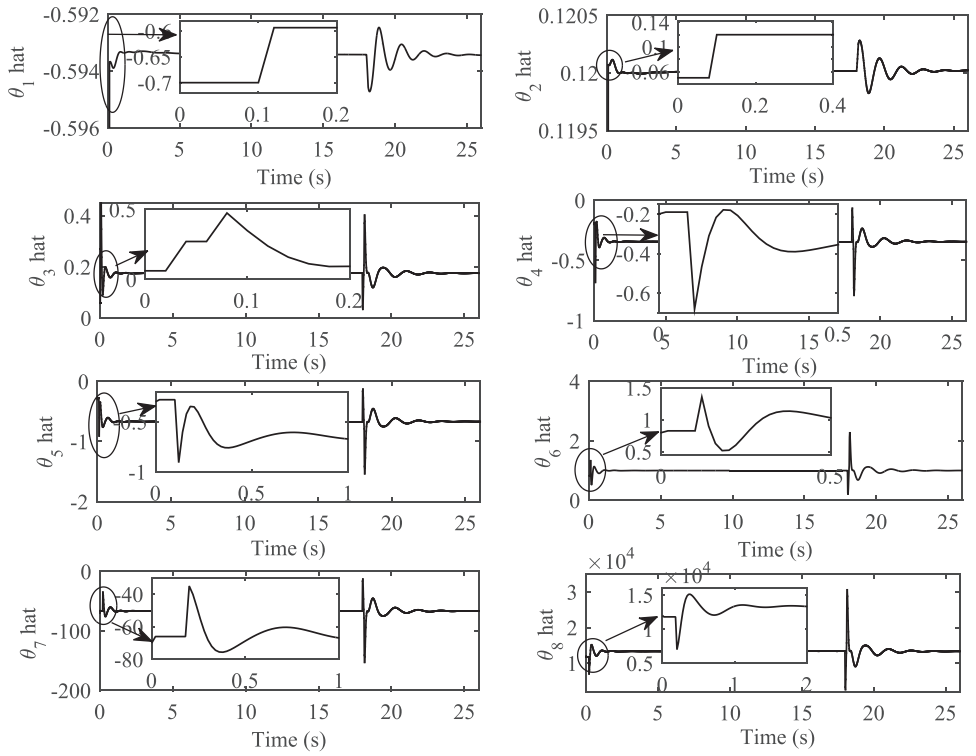

FIGURE 17 Estimated unknown parameters of G4 when the line connecting bus-15 and bus-16 is temporarily disconnected

transients. The small signal-stability analysis is performed for the system in Figure 4 to determine the effects of different synchronous generator on the overall stability of the power system. The modal analysis based on state participation factors of different generators are used in this work for the small-signal analysis. The modal analysis is a well-established method to identify these vulnerable synchronous generators [2]. Based on the small-signal analysis, the vulnerable generators are identified by considering the damping factor. Actually, the generators which have less than 5% damping are considered as critical generators. In this work, the modal analysis performed on the test system in Figure 4 identifies the synchronous generator (G3) at bus-32 and G4 at bus-33 as the most critical generators whose states severely affect the damping of the system. Therefore, the excitation systems of G3 and G4 are considered as the best choices for implementing the designed ABEC. The detailed modal analysis is not presented in this paper as it is out of the scope of this work. Three different situations are considered for validating the effectiveness of the designed ABEC as these situation reflect the operation of the system under different conditions while considering large disturbances. These three situations are captured through following three cases:

- Application of a symmetrical, that is, three-phase 3LG fault at the terminal of a vulnerable generator,
- Application of symmetrical fault at the middle of a key transmission line between two buses, and
- Temporary disconnection of a key transmission line between two buses.

For the first two cases, symmetrical faults, which are also known as the three-phase short-circuit or three line-to-ground (3LG) faults where the system experiences fault at t=18 s which is then cleared at t=18.2 s. Here, the fault duration is considerably larger, that is, 0.2 s which is mainly for demonstrating large disturbances. Comparative results are also presented where the comparisons are made with the EABEC as presented in [30], existing partial feedback linearizing controller (EPFBLC) [17], and existing sliding mode controller (ESMC) [18] for three different operating conditions in three cases. The excitation control laws for the EABEC, PFBLC, and ESMC are not provided here as these can be found from [30], [17], and [18], respectively. Please note that the time-domain results are shown from t=12 s as the responses are in the steady-state and the inclusion of these responses from the beginning will affect the visibility of the responses of interests, that is, few seconds after clearing the temporary faults.

- **Case 1: Effectiveness of the controller for a symmetrical 3LG fault at the terminal of a vulnerable generator**

As discussed earlier in this section, G3 and G4 are determined as the most critical generators affecting the stable operation and the symmetrical 3LG applied at the terminal of one of these generators will assist to assess the performance of the ABEC. It is worth mentioning that the protection system will disconnect the generator from the system during this period due to the application of this fault. Hence, the terminal voltage of G4 will be reduced to zero for the fault duration, that is, from t=18 s to t=18.2 s and the output power generated by this generator will also be zero. At the same time, other responses of G4 (e.g. the speed deviation and rotor angle) will be disturbed but will not be reduced to zero as it takes time to fully stop the rotation of the rotor. Soon after clearing the fault (i.e. at t=18.2 s), G4 will be reconnected with the system through the relay coordination and it will start delivering power into the system. However, the post-fault responses of the system, that is, the terminal voltages, speed deviations, rotor angles, and control signals of other generators will still have oscillating characteristics even after clearing the fault. These oscillations can easily be damped if the excitation controller is more effective. Otherwise, these oscillations will sustain for a while which will make the system unstable.

The terminal voltage responses of few other generators including G4 (i.e. G2, G3, G4, G7, and G10) are shown in Figure 5 from where it can be observed that this becomes zero only for G4 during the fault condition and there are oscillations when the fault is cleared. The terminal voltages of other generators in Figure 5 shows similar post-fault responses though these are reduced to non-zero values for the fault duration. From Figure 5, it is clear that the designed ABEC eliminates the post-fault oscillations in the terminal voltage responses of these generators in a better way than the EABEC, PFBLC, and ESMC. However, oscillating behaviors in the terminal voltage is less severe as compared to other responses as the stability issues are mainly dominated by the angle stability which has direct the relationship with the speed deviation and output active power of the generator. From Figure 6 shows that the synchronous operations of G2, G3, G4, G7, and G10 are disturbed during the fault and the post-fault oscillations in the speed deviations of these generators are effectively damped with the ABEC when the comparisons are with the three other controllers. The severity of the fault can be clearly observed from the rotor angle responses of all these generators as presented in Figure 7. However, the ABEC damps out the post-fault oscillations in a much better way than other nonlinear controllers. The output active power also exhibits similar oscillating behaviors to that of rotor angles which can be observed in Figure 8 though the active power for G4 becomes zero during the fault duration. However, the output active power of other generators does not reduce to zero while it is being severely disturbed as shown in Figure 8. However, the post-fault oscillations are quickly eliminated by the designed ABEC. The excitation control signals for G2, G3, G4, G7, and G10 are shown in Figure 9 which further validate the effectiveness of the ABEC over other excitation controllers as these signals reach to their physical limits during the fault as well as for few cycles even after clearing the fault. However, the stable control signals are finally obtained for exciters in G2, G3, G4, G7, and G10 which are more stable for the scenario when the ABEC is used.

The effectiveness of the ABEC depends on the efficacy of the parameter adaptation laws for estimating unknown parameters. Figure 10 shows the estimated values of unknown parameters which are used as inputs for the excitation control inputs of G4. Similarly, the same parameters are also estimated for G3 as the ABEC for this generator uses similarly estimated parameters. In Figure 10, there are transients at the beginning of the estimation process which are mainly due to the randomness initial values of corresponding unknown parameters. However, the steady-state values of these parameters are easily determined within few seconds. Figure 10 also shows that the parameter estimation process is disturbed at the instance of occurring the fault. However, the adaptation laws efficiently adapt all unknown parameters after clearing the fault which can also be observed from Figure 10.

- **Case 2: Effectiveness of the controller while applying a symmetrical 3LG at the middle of a key transmission line between two buses**

The transmission line between bus-16 and bus-19 can be considered as one of the key transmission line for the test system in Figure 4 as two major synchronous generators (G5 and G4) including a vulnerable one connected with bus-19. In this case, the effectiveness of the ABEC is assessed by applying a symmetrical 3LG fault at the middle of the line connecting these two buses, that is, bus-16 and bus-19 for which the fault sequence is considered as similar to that of the previous case study. The application of this fault will disturb the terminal voltage of G2, G3, G4, G7, and G10 which can clearly be found from Figure 11. Similar responses ad discussed in the previous case (i.e. speed deviations, rotor angles, and control signals) of these four generators will be disturbed that can be evidenced from Figures 12, 13, and 14, respectively. From all these

TABLE 2 Quantitative results for Case 1 in terms of the percentage overshoot and settling time for the speed deviation with different controllers

	PFBLC		ESMC		EABEC		ABEC	
Generator	Percentage overshoot	Settling time (s)	Percentage overshoot	Settling time (s)	Percentage overshoot	Settling time (s)	Percentage overshoot	Settling time (s)
G2	0.5	6.36	0.51	5.8	0.5	2.9	0.094	1.18
G3	0.53	3.92	0.53	5.08	0.9	3.9	0.17	2.78
G4	0.52	5.18	0.32	7.94	0.93	3.66	0.17	2.87
G7	0.94	5	0.945	4.98	0.57	2.82	0.06	1.18
G10	0.52	5.15	0.3	7.37	0.17	3.08	0.11	1.2

responses, severe post-fault oscillations can be observed for vulnerable generators (i.e. G3 and G4) than other generators. The ABEC quickly damps these oscillation in order to ensure the faster settling time as compared to three other nonlinear controllers.

It is necessary to choose the initial values of the unknown parameters before estimating them. In this case study, the initial values are chosen as $\theta_i(0) = (-0.3; 0.15; 0.2; -0.4; -0.8; 1.2; -50; 14000)$ and these initial values are selected based on the nominal values accessible in [33]. As shown in the block diagram, the adaptation laws will now estimate these parameters based on the convergence of desired outputs. It will take some time for the intended outputs to settle down to the values that will allow them to attain their steady-state. As shown in Figure 15, all unknown parameters settle down to their steady-state values after a few seconds. The adaptation gains, which are utilized in the adaptation laws, determine the settling time. The estimation of these parameters will be disrupted when a three-phase short-circuit fault is occurred on the line connecting bus-16 and bus-19, as shown in Figure 15. At t = 18 s, a three-phase short-circuit fault is applied, which is cleared at t = 18.2 s. As soon as the fault is cleared, the estimated parameters return to their pre-fault levels. This clearly demonstrates the superiority of the designed control scheme in estimating unknown parameters.

- **Case 3: Effectiveness of the controller in the case of a temporary disconnection of a transmission line between two-buses**

The transmission line linking two buses, that is, bus-14 and bus-15 is an important line which is temporarily disconnected for 0.2 s. That is the line is tripped at t=18 s while reconnected through the action of the an autorecloser at t=18.2 s. From the observation of the active power flowing through the line, it can be seen from Figure 16 that there is no power flow for the fault duration while there are oscillations after reconnecting the line at t=18.2 s. Figure 16 clearly demonstrates that there are more oscillations when existing nonlinear controllers are used and these oscillations sustain for a longer duration with other controllers.

The initial values of the unknown parameters in this case study are $\theta_i(0) = (-0.7; 0.05; 0.06; -0.2; -0.3; 0.8; -70; 12000)$ which differs significantly from the previous case study. The estimated parameters are presented in Figure 17 from where it can be observed that the estimation takes some time to settle down to the appropriate values for the intended outcomes. The steady-state values in this situation are comparable to those in the prior case. When the line is disconnected for 0.2 s, these estimated values are disrupted but these return to the steady-state when the line is reconnected due to the designed control action. Therefore, it is obvious that the designed controller can estimate unknown parameters under various conditions, including various initial values.

Based on all these comparative results, it can easily be summarized that the ABEC is capable to fully ensure the stable operation during severe transients. Furthermore, the changes in operations do not affect the damping capability of the ABEC even without knowing any parameter within the dynamical model. The quantitative results corresponding to the speed deviations for different generators during the 3LG fault at the terminal of G4 as discussed in Case 1 are shown in Table 2. These are shown in terms of key factors (i.e. the percentage overshoot and the settling time) for evaluating the steady-state behavior of any responses. Table 2 confirms the superiority of the ABEC over other controllers.

6 | CONCLUSIONS

An adaptive backstepping scheme is used to derive the excitation control and parameter adaptation laws considering a more realistic model of synchronous generators. The designed controller has several advantages and one of the major advantages is the utilization of nonlinearities rather than cancelations while another benefit is its is insensitivity to parameter variations. The designed scheme allows to estimate any parameter which is incorporated as the unknown parameter within the dynamical model and there is no requirement of bounding uncertainties. Both excitation control and parameter adaptation laws are determined by guaranteeing the steady-state operation of all properties appeared in the dynamical model. Simulation results over a range of operating conditions reveal that the designed

adaptive excitation controller is more effective while comparing its existing counterparts. The designed controller exhibits faster settling time as it provides more damping than existing controllers which helps the disturbed responses to settle down to their pre-fault steady-state values. As a part of the future work, the proposed scheme will be employed to design coordinated excitation and steam-valve controllers for multimachine power systems in order to tackle large load variations. The future works can also be devoted to design nonlinear state observers so that the states can be directly determined using only the measurement of outputs instead of using algebraic relationships. Moreover, the load is considered as the constant and the dynamic of the mechanical power input representing the dynamic of the turbine-governor system is neglected in this work. Future works will consider this dynamic and analyze the equal area criterion for each fault in order to further demonstrate the effectiveness of the proposed scheme.

ACKNOWLEDGEMENT

The authors would like to thank Deakin University in Australia as a part of this work was carried out during their tenure at Deakin.

FUNDING

None

CONFLICT OF INTEREST

The authors do not have any conflict of interests.

PERMISSION TO REPRODUCE MATERIALS FROM OTHER SOURCES

None

DATA AVAILABILITY STATEMENT

The data that support the findings of this study are available on request from the corresponding author. The data are not publicly available due to privacy or ethical restrictions.

ORCID

Tushar Kanti Roy https://orcid.org/0000-0002-1992-0881
Md Apel Mahmud https://orcid.org/0000-0002-5302-5338

REFERENCES

1. Mahmud, M.A., Hossain, M.J., Pota, H.R.: Investigation of critical parameters for power systems stability with dynamic loads. In: IEEE PES General Meeting, pp. 1–6. IEEE, Piscataway (2010)
2. Kundur, P.: Power System Stability and Control. McGraw-Hill, New York (1994)
3. Dysko, A., Leithead, W.E., O'Reilly, J.: Enhanced power system stability by coordinated pss design. IEEE Trans. Power Sys. 25(1), 413–422 (2010)
4. Majumder, R., Chaudhuri, B., El Zobaidi, H., Pai, B.C., Jaimoukha, I.M.: Lmi approach to normalised H_∞ loop-shaping design of power system damping controllers. IEE Proc. Gen. Trans. Dist. 152(6), 952–960 (2005)
5. Hossain, M.J., Pota, H.R., Ugrinovskii, V.A., Ramos, R.A.: Voltage mode stabilisation in power systems with dynamic loads. Int. J. Elect. Power Eng. Syst. 32(9), 911–920 (2010)
6. Mahmud, M.A., Hossain, M.J., Pota, H.R., Roy, N.K.: Robust nonlinear excitation controller design for multimachine power systems. In: 2014 IEEE PES General Meeting, pp. 1–5. IEEE, Piscataway (2014)
7. King, C.A., Chapman, J.W., Ilic, M.D.: Feedback linearizing excitation control on a full-scale power system model. IEEE Trans. on Power Sys. 9(2), 1102–1109 (1994)
8. Mahmud, M.A., Hossain, M.J., Pota, H.R., Ali, M.S.: Zero dynamic excitation controller design for power system with dynamic load. In: Australasian Universities Power Engineering Conference, pp. 1–7. IEEE, Piscataway (2011)
9. Roy, T.K., Mahmud, M.A., Shen, W., Oo, A.M.T.: Nonlinear excitation control of synchronous generators based on adaptive backstepping method. In: 10th IEEE Conference on Industrial Electronics and Applications, pp. 11–16. IEEE, Piscataway (2015)
10. Fan, B., Yang, Q., Wang, K., Xu, J., Sun, Y.: Transient stability enhancement control of power system with time varying constraints. IET Gener. Transm. Distrib. 10(13), 3251–3263 (2016)
11. Loukianov, A.G., Canedo, J.M., Utkin, V.I., Vazquez, J.C.: Discontinuous controller for power systems: sliding-mode block control approach. IEEE Trans. Ind. Electron. 51(2), 340–353 (2004)
12. Ribeiro, R.L.A., Neto, C.M.S., Costa, F.B., Rocha, T.O.A., Barreto, R.L.: A sliding-mode voltage regulator for salient pole synchronous generator. Electr. Power Syst. Res. 129, 178–184 (2015)
13. Kumar, B.K., Singh, S., Srivastava, S.: A decentralized nonlinear feedback controller with prescribed degree of stability for damping power system oscillations. Elect. Power Syst. Res. 77(3-4), 204–211 (2017)
14. Kenne, G., Goma, R., Nkwawo, H., Lagarrigue, F.L.: An improve direct feedback linearization technique for transient stability enhancement and voltage regulation of power generators. Int. J. Power Energy Syst. 32, 809–816 (2010)
15. Mahmud, M.A., Pota, H.R., Aldeen, M., Hossain, M.J.: Partial feedback linearizing excitation controller for multimachine power systems to improve transient stability. IEEE Trans. Power Sys. 29(2), 561–571 (2014)
16. Mahmud, M.A., Pota, H.R., Hossain, M.J.: Full-order nonlinear observer-based excitation controller design for interconnected power systems via exact linearization approach. Int. J. Electr. Power Energy Syst. 41(1), 54–62 (2012)
17. Mahmud, M.A., Hossain, M.J., Pota, H.R., Oo, A.M.T.: Robust partial feedback linearizing excitation controller design for multimachine power systems. IEEE Trans. Power Sys. 32(1), 3–16 (2017)
18. Colbia Vega, A., de Leon Morales, F.L. J., Pena, O.S., Mata Jimenez, M.T.: Robust excitation control design using sliding-mode technique for multimachine power systems. Electr. Power Syst. Res. 78(9), 1627–1634 (2008)
19. Loukianov, A.G., Canedo, J.M., Fridman, L.M., Soto Cota, A.: High-order block sliding-mode controller for a synchronous generator with an exciter system. IEEE Trans. Ind. Electron. 58(1), 337–347 (2011)
20. Roy, T.K., Mahmud, M.A., Shen, W.X., Oo, A.M.T., Haque, M.E.: Robust nonlinear adaptive backstepping excitation controller design for rejecting external disturbances in multimachine power systems. Int. J. Elect. Power Eng. Syst. 84, 76–86 (2017)
21. Roy, T.K., Mahmud, M.A., Shen, W.X., Oo, A.M.T.: Non-linear adaptive coordinated controller design for multimachine power systems to improve transient stability. IET Gener. Transm. Distrib. 10(13), 3353–3363 (2016)
22. Roy, T.K., Mahmud, M.A., Shen, W., Oo, A.M.T.: Nonlinear adaptive excitation controller design for multimachine power systems with unknown stability sensitive parameters. IEEE Trans. Control Syst. Technol. PP(99), 1–13 (2017)
23. Meng, W., Wang, X., Fan, B., Yang, Q., Kamwa, I.: Adaptive non-linear neural control of wide-area power systems. IET Gen. Transm. Distrib. 11(18), 4531–4536 (2017)
24. Mitra, A., Mukherjee, M., Naik, K.: Enhancement of power system transient stability using a novel adaptive backstepping control law. In: Proceedings of IEEE Third International Conference on Computer, Communication, Control and Information Technology, pp. 1–5. IEEE, Piscataway (2015)
25. Wang, B., Shi, Z.: Backstepping adaptive variable structure excitation controller for multimachine power system. In: International Conference on Electrical and Control Engineering, pp. 88–91. IEEE, Piscataway (2011)

26. Fu, J., Zhao, J.: Robust nonlinear excitation control based on a novel adaptive backstepping design for power systems. In: Proceedings of American Control Conference, pp. 8–10. IEEE, Piscataway (2005)
27. Roy, T.K., Mahmud, M.A., Shen, W., Oo, A.M.T.: Nonlinear adaptive excitation controller design for multimachine power systems. In: Proceedings of IEEE PES General Meeting, pp. 1–5. IEEE, Piscataway (2015)
28. Roy, T.K., Mahmud, M.A., Oo, A.M.T., Haque, M.E.: Robust adaptive excitation control of synchronous generators in multimachine power systems under parametric uncertainties and external disturbances. In: Proceedings of the 56th IEEE Conference on Decision and Control. IEEE, Piscataway (2017)
29. Wan, Y., Jiang, B.: Practical nonlinear excitation control for a single-machine infinite-bus power system based on a detailed model. Automatica 62, 18–25 (2015)
30. Roy, T.K., Mahmud, M.A., Oo, A.M.T.: Robust adaptive backstepping excitation controller design for higher-order models of synchronous generators in multimachine power systems. IEEE Trans. Power Sys. 34(1), 40–51 (2019)
31. Roy, T.K., Mahmud, M.A., Oo, A.M.T., Pota, H.R.: Nonlinear adaptive backstepping excitation controller design for higher-order models of synchronous generators. IFAC-PapersOnLine 50(1), 4368–4373 (2017)
32. Pai, M.A., Sauer, P.W., Lesieutre, B.C.: Static and dynamic nonlinear loads and structural stability in power systems. Proc. IEEE 83(11), 1562–1572 (1995)
33. Pai, M.A.: Energy Fuction Analysis for Power System Stability. Kluwer, Boston, MA (1989)

How to cite this article: Roy, T.K., Mahmud, M.A.: A nonlinear adaptive excitation controller design for two-axis models of synchronous generators in multimachine power systems to augment the transient stability during severe faults. IET Gener. Transm. Distrib. 16, 3906–3927 (2022).
https://doi.org/10.1049/gtd2.12575